INFILTRATION EFFECTS ON CROSS-SHORE SEDIMENT TRANSPORT

by

Trevor Ross Elliott

B.Sc.(Eng.), Queen's University, 1993

A THESIS SUBMITTED IN PARTIAL FULFILLMENT OF

THE REQUIREMENTS FOR THE DEGREE OF

MASTER OF APPLIED SCIENCE

in

THE FACULTY OF GRADUATE STUDIES

DEPARTMENT OF CIVIL ENGINEERING

We accept this thesis as conforming

to the required standard

THE UNIVERSITY OF BRITISH COLUMBIA

October, 1995

In presenting this thesis in partial fulfilment of the requirements for an advanced degree at the University of British Columbia, I agree that the Library shall make it freely available for reference and study. I further agree that permission for extensive copying of this thesis for scholarly purposes may be granted by the head of my department or by his or her representatives. It is understood that copying or publication of this thesis for financial gain shall not be allowed without my written permission.

Department of Civil Engineering

The University of British Columbia
Vancouver, Canada

Date 14 OCT 95

DE-6 (2/88)

ABSTRACT

Theory is reviewed which relates infiltration into a permeable beach with the net onshore or offshore transport of sediment by wave action. This theory is tested experimentally by using sands of different permeability and by using underdrains in the beach and a pump to increase the infiltration capacity. Previous studies are reviewed, although these earlier studies have had different purposes. Some prior investigations have studied wave propagation over a permeable slope or have determined wave damping and energy dissipation due to percolation into a porous bed. Other studies have investigated wave interactions with permeable structures such as rubblemound breakwaters and have shown that the exchange of fluid between the external and internal flow regions markedly affects wave uprush, backrush and set-up in the surf zone. A limited number of previous studies have considered the flow of fluid into a permeable beach and its role in beach stabilization and erosion control. The present tests were performed in the wave flume of the Hydraulics Laboratory of the Department of Civil Engineering at the University of British Columbia. Intermediate and equilibrium beach profiles are presented and compared. The findings of this study indicate substantial differences between impermeable and porous material. Experimental results show more permeable beaches form steeper profiles, while less permeable beaches form shallower profiles. Moreover, increasing infiltration by pumping initiates immediate onshore sediment motion and considerable steepening of the cross-sectional profile. To a large extent this steepening process was reversible when pumping was stopped. The results of this study confirm the predictions of the theory that infiltration contributes directly to a net onshore stress and onshore sediment transport.

Table of Contents

List of Tables

List of Figures

List of Symbols

a	Wave amplitude
b	Turbulent coefficient for Forchheimer Equation
C	Constant value
c	Added mass coefficient in Forchheimer Equation
D	Grain size
d	Bed thickness
E	Wave Energy
G	Shear Modulus
GMε	Geometric Mean Grain Diameter
g	Gravitational Acceleration
H	Wave Height
h	Local Water Depth
k	intrinsic permeability
K	Hydraulic conductivity
K_r	Reflection Coefficient
L	Wavelength
l	Half the Length of surf zone from break-point to maximum run-up
m	Stiffness ratio $\frac{nG}{(1-2\upsilon)\beta}$
n	Ratio between group velocity and celerity, porosity
P	Total Pressure
p	Excess Pressure
p_o	Excess Pressure at sea bed interface
q	Flow velocity in porous medium
S	Total radiation stress
S_{xx}	Excess radiation stress
s	hydraulic gradient
T	Wave Period
t	Time
u	Velocity in x direction
v	Velocity in y direction
w	Velocity in z direction
x	Horizontal
y	Longshore
z	Vertical
α	Local bed slope angle
β	Fluid-Air compressibility
δ	Boundary Layer Thickness
ε	Phase angle
ε_r	Phase between reflected and incident wave
ϕ	Potential function
γ	Breaker Index

η	Angular coordinate in elliptical system
υ	Poisson's Ratio
θ	$2\pi\left(\frac{x}{L}-\frac{t}{T}\right)$
ρ	Fluid Density
σ'	Effective Stress
σ_ϕ	Sediment-size Standard Deviation in Phi Units
τ	Shear Stress
ξ	Spatial coordinate in elliptical coordinate system
ψ	Stream function
ζ	Vertical coordinate of water surface

Acknowledgements

The author sincerely thanks Dr. Michael Quick for his guidance and insight throughout this project. His enthusiasm and interest were greatly appreciated. Thanks also to Mr. Kurt Nielsen for his expertise, advice and patience. The input and ingenuity of Mr. Ron Dolling and Mr. John Wong are also recognized. The author is grateful to the following graduate students who were instrumental in their teachings, discussions and friendship: Amal Phadké, Jason Vine, Wayne Evans and John Wilkinson.

The generous financial support from NSERC is also gratefully acknowledged.

Chapter 1

Introduction

1.1 General

Beaches are a form of "soft" shore protection that dissipate wave energy, and act as protective barriers between fierce ocean storms and otherwise vulnerable property. Variations in seasonal conditions and individual storm events move tons of material across the surf zone annually.

It is well recognized and generally accepted that beaches comprised of coarse material, such as cobble and gravel are steeper than fine grained shores. The correlation between particle size and hydraulic conductivity indicates that increased permeability and improved infiltration capacity are contributing to the steeper slopes of these stable shores.

Quick (1991) has shown that it is the increased infiltration from improved hydraulic conductivity that contributes to a net onshore stress and results in steeper slopes. Results from some small scale tests (Quick and Dyksterhuis, 1994) indicate that the fine sediment fraction controls the material permeability and has a controlling influence on the equilibrium profile. These initial experiments pointed out the need for larger scale testing on a greater range of sediment mixtures.

Little other work has been done to determine the effect of infiltration and exfiltration from the beach face on the equilibrium beach profile. This thesis describes the findings from a mobile bed hydraulic model study investigating these effects.

The role of infiltration in controlling the beach slope was illustrated in two different ways. One experiment used sand and gravel mixtures with different gradations to investigate the effect of changing the bed permeability; while another used a pumped drain system under the beach to artificially induce infiltration. The equilibrium profiles were analyzed to compare the stable beach angle for these different infiltration conditions. The findings from such an investigation will provide coastal engineers with guidance when evaluating the impact of artificial nourishment using beach fill of different permeability than the native material. Realizing the importance of infiltration and its effects on surf-zone dynamics will lead to a better understanding of coastal processes and improved shoreline prediction.

1.2 Literature Review

Researchers have long realized the importance of permeability and infiltration and their role in beach formation and coastal erosion. Perhaps the first to describe beach formation by waves was Bagnold (1941). In this early account, Bagnold developed and formulated "the percolation hypothesis" from his observations of what could be one of the earliest accounts of scale modeling in coastal hydraulics. Bagnold reported that velocities normal to the bed are appreciable and steady during the uprush, backrush and especially at the instant when the surge is momentarily stopped having reached its maximum height and about to retreat back down the slope. Water continues to flow downward into the porous beach, reducing the volume of water available to participate in the backrush. The return surge is responsible for offshore sediment movement. Bagnold also noted that the prevention of free percolation contributes to the breakdown and flattening of an otherwise steep beach that is stable and in equilibrium. Bagnold verified this claim by a simple and convincing experiment where an impervious steel plate was

inserted beneath the beach face. Thin layers of material above the plate became unstable and were removed as the beach adjusted to a reduced equilibrium slope.

Bagnold reasoned that potential energy lost by percolation of water into the bed was greater for material of high porosity. This energy loss made the uprush stronger than the backrush and made onshore sediment drag larger. The backrush cycle, which is associated with down slope movement of material, is weakened and its ability to drag sediment offshore reduced. The increased energy dissipated by coarse beaches is responsible for steeper slopes than would be stable for impermeable beaches on which uprush and backrush energy differ only by energy lost to bottom friction and turbulence. Bagnold called this effect the "porosity increment". Similar arguments were presented in Inman and Bagnold (1963).

Longuet-Higgins and Parkin (1962) concluded that reduced percolation over an impermeable layer increases the power of the waves to move the overlying material. In an investigation into the formation of beach cusps, the authors determined that an impermeable sand shingle mixture below the bed surface in the bays promotes instability. The promontories, composed of well-sorted shingle, were more stable apparently because of their high permeability and greater porosity. The relative hydraulic conductivity of these two different formations was determined by two simple experiments. One test measured the time required for water to percolate into the material when poured down a permeameter; while another measured the time required for water to infiltrate into the ground when poured on the surface of each individual feature. Longuet-Higgins and Parkin concluded that greater permeability improved the likelihood of constructive action by waves.

King (1972) argued that the down-slope component of the force of gravity balances the force of the swash and backwash. On a shingle beach, where the uprush is considerably stronger

than the backrush, a steeper slope increases the down-slope component of gravity increasing its effectiveness and its ability to maintain equilibrium.

Collins and Chesnutt (1975) studied the effect of grain size distribution on equilibrium beach profiles. They report that for a bimodal distribution, the bar is formed farther offshore, and the slope is also different. This supports the premise that material composition affects the natural equilibrium profile.

Gourlay (1980) recognized the importance of classifying beach sediment by their permeability and other similar hydraulic properties such as fall velocity and fluidizing velocity. Gourlay concluded that the fluidizing velocity is very important when determining the profile shape and presented the relationships between the fluidizing velocity, permeability and fall velocity. Gourlay non-dimensionalized the fall velocity with deepwater wave height and period (H_o/v_fT) to yield a parameter that is well known and has been widely used by many researchers for profile and erosion prediction.

Sleath (1984) also realized the role of permeability in bed fluidization and grain instability but also discusses the effect that flow into and out of the bed has on the boundary layer, bed shear, and incipient motion. Seepage modifies the fluid flow in the boundary layer which changes the shear stress on the bed, and also affects the laminar-turbulent boundary layer transition.

1.3 Scope of Present Work

The preceding work shows that infiltration is clearly important and illustrates some effects it can have on sediment transport processes. A definitive investigation is required to

determine more clearly the effect of infiltration on the beach profile and confirm by experiment the predictions of earlier theoretical analysis.

The purpose of this study is to investigate the influence of infiltration on cross-shore sediment transport and its effect on the equilibrium slope and profile. An experimental model study was conducted using two hydraulic models. One experiment involved the use of sand mixtures of different gradations to investigate the effect of changing bed permeability, while the other used a pumped drain under the beach face to increase infiltration. The profiles at intermediate and equilibrium stages were analyzed to compare the stable slope angle and beach length within the surf zone for different infiltration conditions. Included in the profiles were also the recorded changes to distinctive features such as erosion of the beach berm and enlargement of the breaker bar.

Chapter 2

Background Theory and Governing Equations

2.1 Shallow-water Long Wave Equations

The motivation of this work is derived from the theoretical treatment of cross-shore sediment transport and infiltration that contributes to an onshore bed shear stress described in detail by Quick (1991), and more generally in Quick and Dyksterhuis (1994).

A surf zone fluid element is shown in Figure 2.1. The horizontal velocity is depth averaged and vertical velocity gradients are therefore assumed to be negligible. Under these conditions, the pressure can be assumed to be hydrostatic. The vertical pressure gradient at the interface is assumed to dominate and infiltration into the beach face is thus assumed to be predominantly vertical. The free surface elevation varies with time and shoreward position.

For this system, the equations of continuity and momentum are:

$$\text{Continuity: } \frac{\partial}{\partial x}(hu)+\frac{\partial h}{\partial t}=-q_z \qquad [1.1]$$

$$\text{Momentum: } \frac{d}{dt}(\rho h\cdot\delta x\cdot u)=-\tau_b\cos\alpha\cdot\delta x-\rho gh\left(\frac{\partial h}{\partial x}\delta x+\frac{\partial z}{\partial x}\delta x\right). \qquad [1.2]$$

$$\text{Where } \frac{\partial h}{\partial x}=\frac{\partial \zeta}{\partial x}-\frac{\partial z}{\partial x}. \qquad [1.3]$$

τ_b is the onshore shear stress at the bed; q_z is the vertical infiltration velocity; and ζ is the displacement of the water surface relative to the still water line. The local water depth is h; u is the local depth averaged horizontal velocity; and α is the local bed slope angle. The horizontal

and vertical coordinate axes are x and z respectively; t is time; ρ the fluid density, and g is gravitational acceleration.

Expanding and rearranging Equation [1.3] yields:

$$\frac{\tau_b}{\rho}\cos\alpha = -gh\frac{\partial\zeta}{\partial x} - \left[u\left(h\frac{\partial u}{\partial x} + u\frac{\partial h}{\partial x} + \frac{\partial h}{\partial t}\right) + h\frac{\partial u}{\partial t}\right]. \qquad [1.4]$$

Substituting the continuity relationship where it appears in the momentum equation and time averaging, the time derivative of velocity vanishes to give the final expression for the bed shear stress.

$$\frac{\tau_b}{\rho}\cos\alpha = -gh\frac{\partial\bar{\zeta}}{\partial x} + \overline{uq_z} \qquad [1.5]$$

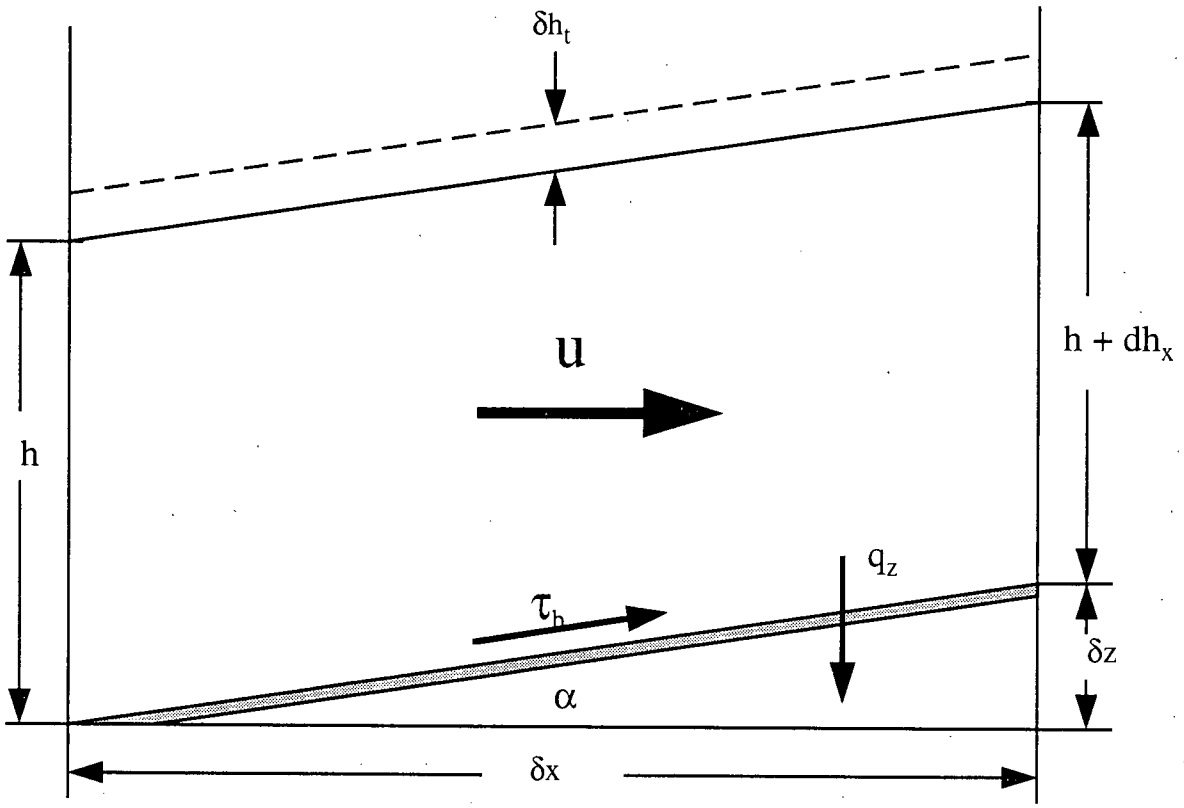

Figure 2.1 Fluid Element and Control Volume

The large number of waves required to produce lasting changes to the coast justify the time averaged approach. The product of the local depth averaged velocity and the infiltration velocity contributes to a net onshore stress.

The infiltration velocity is normally assumed to be in-phase with the wave induced bottom pressure which is in phase with the disturbance at the free surface. If the horizontal velocity and infiltration velocity are out of phase by an angle ε, the mean value of the infiltration induced shear stress, τ_i, is proportional to the product of two cosine functions averaged over the wave cycle.

$$\overline{\tau}_i \propto \frac{1}{2\pi}\int_0^{2\pi} \cos\theta \cos(\theta+\varepsilon) d\theta \qquad [1.6]$$

Simplification using trigonometric identities and integration yields:

$$\overline{\tau}_i \propto \frac{1}{2}\cos\varepsilon \qquad [1.7]$$

Thus, the time averaged infiltration induced shear stress is sensitive to the phase relationship between the flow velocity and the infiltration velocity. In phase velocities generate a maximum onshore stress; while out of phase velocities can produce a zero net shear or even a complete reversal to offshore stress.

The applicability of this theory is conditional on the assumptions made in its development. Linear wave theory predicts that fluid velocities in shallow water will be predominantly horizontal and uniform throughout the depth of flow. For oscillatory flow in shallow water, the boundary layer is most likely thin enough that it can be neglected. The shallow water restriction substantiates the presumption of hydrostatic pressure as the only logical

choice. It will be shown later that fluid flow across the interface can be assumed to be predominantly normal to the bed.

Similar long wave equations have been presented by van Gent (1994) in which the term qq_x is improperly added to the otherwise correct equation of momentum. Van Gent justifies the equation by arguing that the exchange of fluid between the external and internal regions is a transfer of momentum and a condition that necessitates a force. His rationalization is correct, although the transfer of momentum is a consequence of continuity.

2.2 Radiation Stress

To evaluate the first term on the right hand side in Equation [1.5], which is an offshore stress and remnant from the assumption of hydrostatic pressure, it is necessary to evaluate the wave-induced set-up. This was done by Longuet-Higgins and Stewart (1964) employing the radiation stress concept that evaluates the excess momentum due to the presence of the waves from linear wave theory predictions. The formulation is presented in more detail in an earlier paper, Longuet-Higgins and Stewart (1962).

The value of the radiation stress including wave reflection for direct wave attack (normal to the shoreline) is given by McDougal et al (1994):

$$S_{xx} = (E_{ii} + E_{rr})\left(2n - \frac{1}{2}\right) - E_{ir}\cos\left(4\pi\frac{x}{L} + \varepsilon_r\right), \qquad [2.1]$$

where x is the distance seaward from the reflective boundary and ε_r is the phase angle between the reflected and incident waves. The incident and reflected wave energy densities are E_{ii} and E_{rr} respectively. The wavelength is given by L; and n is the ratio between the group velocity

and celerity. E_{ir} is $\frac{1}{8}\rho g H_i H_r$, where H_i and H_r are the incident and reflected wave heights respectively.

The above equation indicates that increased energy from wave reflection increases the Radiation Stress which will in turn increase the onshore shear stress at the bed. The authors also note that the reflected waves contributes to a modulation in the set-up as indicated by the second term on the right hand side of Equation [2.1].

When reflection is negligible, the above expression reduces to the well-known relationship given more than thirty years ago by Longuet-Higgins and Stewart (1962):

$$S_{xx} = E\left(2n - \frac{1}{2}\right), \qquad [2.2]$$

where E is the energy density equal to $\rho g \frac{H^2}{8}$ from small amplitude theory.

2.2.1 Set-up and Set-down

Changes in the mean water level from ocean waves propagating into water of gradually varying depth have been explained by Longuet-Higgins and Stewart (1962 and 1964). The formulation was intended for mild slopes where the water depth varies gradually with horizontal distance. Wind stress was not included even though it can cause changes in the water level of the same order as wave induced set-up.

Assuming no flow normal to the beach face, Longuet-Higgins and Stewart equate the horizontal component of the normal force generated by the bottom pressure to the change in total momentum.

$$\frac{\partial S}{\partial x} = \overline{P_o}\frac{dh}{dx} \qquad [2.3]$$

S is the total momentum flux; and $\overline{P_o}$ is the mean total bottom pressure.

From continuity and subtracting the effect of hydrostatic pressure, the change in excess momentum is:

$$\frac{1}{\rho}\frac{\partial S_{xx}}{\partial x} = -g\left(h+\overline{\zeta}\right)\frac{\partial \overline{\zeta}}{\partial x} + \frac{dh}{dx}\left[\int_{-h}^{0}\frac{\partial}{\partial x}\left(\overline{uw}\right)dz - \left(\overline{w^2}\right)_{z=-h}\right] \qquad [2.4]$$

Longuet-Higgins and Stewart neglect terms involving the vertical velocity, w, since it is of order $u\frac{\partial h}{\partial x}$ for an impermeable bed. For that simplifying condition, the mean bottom pressure is equal to mean hydrostatic pressure. This may not be the case for permeable beaches that attract additional stresses. The general theoretical relation for changes in mean water level is well known:

$$\frac{\partial S_{xx}}{\partial x} = -\rho g\left(h+\overline{\zeta}\right)\frac{\partial \overline{\zeta}}{\partial x}. \qquad [2.5]$$

Longuet-Higgins and Stewart (1962) note that: $-\frac{\partial S_{xx}}{\partial x}$ is a horizontal force applied to the fluid that produces a slope to the water surface. Whitham (1962) made an equivalent statement remarking that $\frac{\partial S_{xx}}{\partial x}$ is a force on the step. The convergence of opposing currents driven by sloping water surfaces has been credited as one possible explanation for the formation of the breaker bar (Longuet-Higgins, 1983).

The validity of the general differential equation, Equation [2.5], is independent of shoreward location. It holds in deepwater, shoaling water, and in the surf zone. Waves moving through these regions undergo changes in specific energy, group velocity and celerity. Naturally the value of the Radiation Stress changes accordingly.

Prior to breaking, wave energy is approximately conserved. Thus, changes in momentum are primarily due to changes in the group velocity parameter and a diminishing relative depth. Momentum steadily increases as waves propagate into shallower water in which case the depression of the mean surface can be directly computed from Equation [2.5] or from its integrated form:

$$\overline{\zeta} = -\frac{1}{8}\frac{H^2 \frac{2\pi}{L}}{sinh\frac{4\pi h}{L}}. \qquad [2.6]$$

The above expression is in terms of local wave amplitude and wave length; Longuet-Higgins and Stewart offer an alternate equation involving deepwater parameters. The asymptote in shallow water is:

$$\overline{\zeta} = -\frac{\pi}{16}\frac{{H_0}^2}{L_o}\left(2\pi\frac{h}{L_o}\right)^{-\frac{3}{2}}. \qquad [2.7]$$

Measured values of set-down seaward of the break point presented in Bowen et al (1968) show excellent agreement with the predictions of Longuet-Higgins and Stewart. The depression of the water surface outside the breakpoint is very real, yet overshadowed by the elevation of the mean level within the surf zone. Set-down steadily increases as the waves propagate into progressively shallower water until the waves break. Shoreward energy dissipation from wave breaking decreases radiation stress and, according to Equation [2.5], generates a positive gradient in the time averaged water surface. In shallow water, wave induced set-up is very nearly proportional to the shoreward reduction of specific energy which depends on the shoreward reduction in local wave height. There is however, no reliable theory to accurately predict wave properties after breaking. We must therefore rely on empirical observations and experience.

Broken waves have been modeled with some success as turbulent bores that maintain a constant ratio, γ , between wave height and local depth.

$$H = \gamma\left(\overline{\zeta} + h\right) \qquad [2.8]$$

Longuet-Higgins and Stewart (1964) and Bowen et al (1968) made this assumption of a constant breaker index. This seems an appropriate simplification considering the dynamics of wave breaking is to this day not well understood. The gradient of the water surface was originally proportional to the shoreward derivative of wave height but it can be shown to be proportional to the local rate of change of water depth. For a plane beach, shallow-water setup is constant and proportional to beach slope,

$$\frac{\partial \overline{\zeta}}{\partial x} = -\frac{1}{1+\frac{8}{3\gamma^2}}\frac{dh}{dx} \qquad [2.9]$$

in which it should be noted that in shoaling water, $\frac{dh}{dx}$ is negative.

The breaker index, γ, varies slightly with wave period: but a value of unity seems reasonable from the work of Bowen et al (1968). Their experimental measurements of time averaged water surface elevations using damped manometers show good agreement with the above theory and support the use of a breaker index and the proposed linear relationship between water depth and wave height.

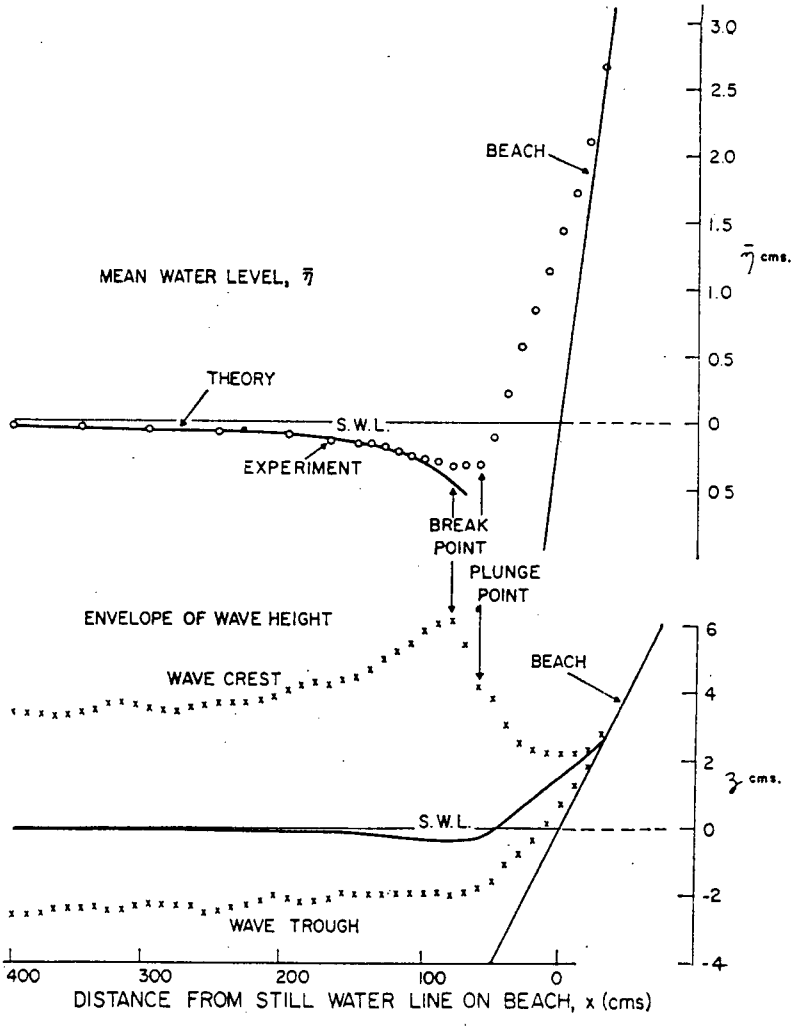

Figure 2.2 Mean Water Level and Wave Height Envelope, Bowen et al (1968)

2.3 Infiltration and Permeability

2.3.1 Darcy's Law

Darcy's law describes a linear relationship between specific discharge of fluid from a permeable body and the pressure gradient required to generate such a flow. The constant of proportionality describing the ease of fluid flow through the porous medium is known as the hydraulic conductivity. The specific discharge, $\mathbf{q}$, also known as the Darcy velocity and "filter" velocity, is a vector having both magnitude and direction.

$$\mathbf{q} = \nabla\phi = -K\nabla\frac{p}{\rho g} \qquad [2.10]$$

The fluid potential, ϕ, is a function of the excess pore-pressure, p, and the material permeability, K, which has the units of velocity.

For most fine beach material, flow velocities are sufficiently small that the velocity head can be neglected. When the flow is predominantly vertical and the pressure is approximately hydrostatic, the equation takes the more familiar form of Darcy's Law:

$$\mathbf{q}_z = -K\frac{\partial h}{\partial z}. \qquad [2.11]$$

In this case, h is the hydraulic head.

For the case of a permeable sea bed underlying water of uniform depth, only pore-water pressures above hydrostatic will produce a dynamic effect. Hydrostatic pressures must be subtracted from the total pore water pressure at any point in the bed. For the coordinate system used in Figure 2.3, the appropriate equation is:

$$\mathbf{q} = -K\nabla\left[\frac{P}{\rho g} - (h + z)\right]. \qquad [2.12]$$

P is the total pressure; z is the depth into the bed of thickness d; and h the local water depth.

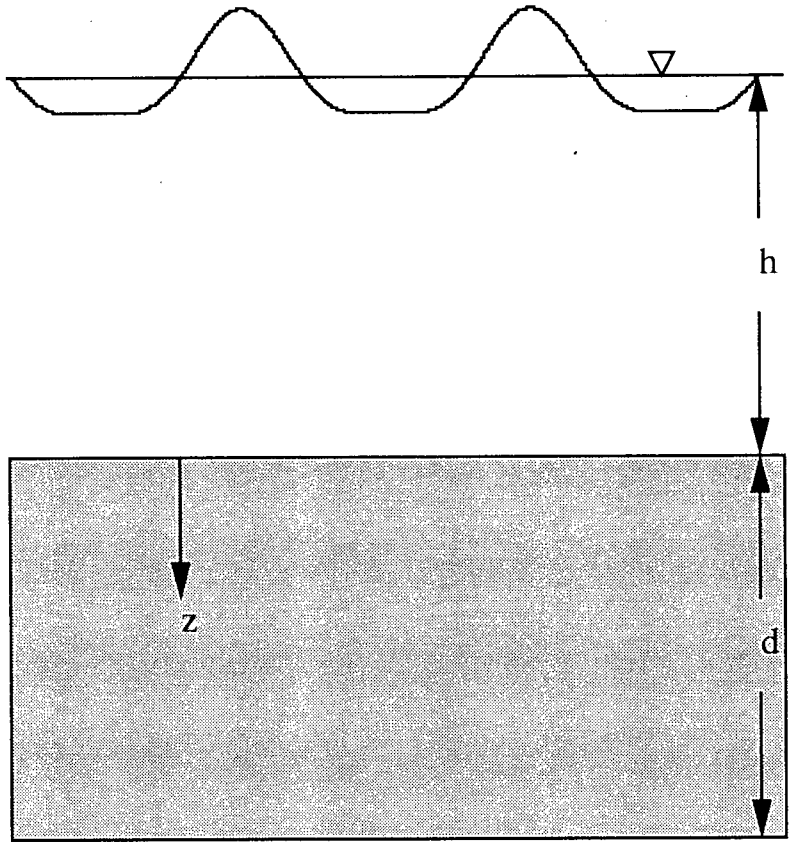

Figure 2.3 Definition Sketch and Coordinate System

2.3.2 Non-Darcy Flow in Porous Media: the Forchheimer Equation

The fluid contained within the interstices of a porous body can be made to move under the application of a driving force. Thus, it is useful to resolve the condition into an equilibrium of driving forces and resisting forces (see for example Hannoura and Barends, 1981). Darcy's law applies only to steady flow in the laminar region where resistance to flow is predominantly

by internal friction and viscous forces. For turbulent flow (analogous to the turbulent region encountered at high Reynolds numbers in pipe flow) or semi-turbulent flow in the transition region, the flow is unsteady and is characterized by large inertial forces from local and convective accelerations. These accelerations generate additional resistance to fluid flow. The aforementioned force balance, which can be extended to include these resistance forces, can be used to predict the non-linear relationship between flow velocity and gradient. One such equation is:

$$\frac{1}{\rho g}\nabla p = -\frac{1}{K}\mathbf{q} + b|\mathbf{q}|\mathbf{q} \qquad [2.13]$$

A relationship of this form was first proposed by Forchheimer (see Hannoura and Barends, 1981) for whom the equation is named. An additional unsteady term, $c\frac{\partial \mathbf{q}}{\partial t}$, can be added to account for the effect of added mass in unsteady flow. The coefficients b and c are not dimensionless.

For most beaches made of fine sand or gradations containing large quantities of very fine material, the fluid flow is most likely to be laminar and obey Darcy's law. Within rubblemound breakwaters, the flow will surely be in the turbulent regime and unsteady effects will exist. Evidently there must be a transition between these two extreme conditions.

2.3.3 Expressions Relating Grain Size and Sorting to Permeability

A porous body has voids filled to some degree with a fluid be it water, air or other. The flow of fluid in a porous medium depends not only on the size of these openings but also their connectivity and distribution throughout the body.

Permeability testing on granular materials is often costly and unreliable because of the difficulty in obtaining undisturbed samples (Gaythwaite, 1990). Hydraulic conductivity can be deduced from particle size distributions obtained from a sieve analysis of a disturbed sample. Permeability and grain size are quite obviously interrelated and empirical relationships have been suggested by many researchers.

Hazen (1911) proposed a relationship for material ranging from fine sand (0.1 millimeters) to fine gravel (3 millimeters).

$$\text{Velocity of flow (ft day}^{-1}) \; v = 8200 D^2 s \qquad [2.14]$$

D is the effective particle size in millimeters, which Hazen selected as the D_{10}, and s is the slope of the ground water table or hydraulic gradient. The coefficient was not constant but varied with the uniformity of the sample. Hazen suggested different values depending on the character and cleanliness of the sand indicated by the uniformity coefficient. For example, Hazen remarked that there was no reason that gravel should follow the formula given for sand. Hazen also noted that the velocity varied with the square root of the head for gravels. Hazen had obviously been aware of the influence of gradation and non-linear effects of non-Darcy flow.

Equation [2.14] describes the flow velocity in the pores, also known as the seepage velocity. The specific discharge or Darcy velocity is averaged over the cross section by assuming an appropriate value for the porosity of the material. Assuming an approximate porosity of 0.4, Equation [2.14] becomes:

$$K\,(\text{ms}^{-1}) = 0.01 D_{10}{}^2 . \qquad [2.15]$$

Krumbein and Monk (1942) also found an empirical correlation between particle size and permeability but extended their investigation to include sediment gradation as well. The equation as it was originally presented is:

$$k\,(\text{darcys}) = 760 GM\varepsilon^2 \cdot e^{-1.31\sigma_\phi}. \qquad [2.16]$$

The geometric mean diameter is $GM\varepsilon$; and σ_ϕ is the sediment-size standard deviation in phi units. Krumbein and Monk used the phi system and specified representative particle diameters by the "percent coarser" convention. The above equation is awkward and has not received much attention as a result. The original equation can easily be transformed into a simpler, more valuable expression.

$$K\,(\text{ms}^{-1}) = 0.00745 \cdot {D_{50}}^2 \left(\frac{D_{16}}{D_{84}}\right)^{0.945} \qquad [2.17]$$

The equation is more useful since particle sizes are expressed as "percent finer" and the relation is clear and simple. One can see that the permeability is approximately proportional to the gradation of the material and the square of the representative grain size.

Chapter 3

Wave Induced Pressure Gradients in Porous Media and Infiltration Effects

3.1 Wave Induced Pressure Gradients and Excess Pore-pressures

Fluid velocity components above the bed are easily determined from an appropriate wave theory. However, most wave theories assume no flow normal to the bottom which makes them unsuited for prediction of the infiltration velocity at the sea bed. Thus to determine the magnitude of the onshore shear stress attributed to infiltration at the interface, the relationship between the wave conditions at the free surface and pressures within the porous bed must be established by alternate means. The estimate of the bottom pressure from most wave theories is still valid and reliable despite the assumption of no-flow into the bed. From the wave-induced pore-water pressures, or more specifically the gradient of excess pore pressure, the flow velocities at the interface can be determined by Darcy's law.

The question remains whether it is the instantaneous pressure fluctuations apparent with the passage of each individual wave, or the time averaged quasi-steady-state infiltration that is more significant. These can be observed in the laboratory by the injection of dye into the beach.

3.2 Transient Pressure Field and Instantaneous Effects

Many investigators have dealt with the problem of wave-induced pore-pressures in porous sea beds. Each solution has a particular application depending on the approach taken and the assumptions that were made. The assumption of a plane horizontal bed and the validity of Darcy's law is common to most. For sandy beaches, the assumption of Darcian flow is most likely justified.

3.2.1 Regular Waves for Infinite and Finite Depth Sea Beds

Sinusoidal waves and the effect of a harmonic pressure disturbance over a plane horizontal sea bed is the most common case studied and reported in the literature. The popularity of this approach is probably linked to the widespread usage of linear wave theory. Algebraic manipulation is uncomplicated by higher order terms, and results are simple and easy to use. The motivation was most likely to provide insight into geotechnical problems such as the stability of offshore drilling platforms and pipelines buried beneath the ocean floor. For an excellent summary see Finn et al (1983).

It is possible to make use of these solutions, keeping in mind their simplifying assumptions, and apply them to shallower water than they were probably originally intended. Although most solutions were presumably not meant to be used in the surf zone, limitations on water depth are not specified. However, some solutions assume or require that the effective vertical and shear stresses at the bed are small. Nonetheless, this has not prevented some researchers from applying these equations to gently sloping beaches (see for example Putnam, 1949, and Sakai et al, 1992b).

Putnam (1949) assumed incompressible flow and therefore ended up solving the Laplace equation. The equation for wave induced pore-pressures in an isotropic finite depth sea-bed is:

$$\left|\frac{p}{p_o}\right| = \frac{\cosh\frac{2\pi}{L}(d-z)}{\cosh\frac{2\pi d}{L}}, \qquad [3.1]$$

where p_o is the wave induced pressure at the sea-bed interface.

Differentiation with respect to z yields the expression for the vertical pressure gradient.

$$\frac{\partial p}{\partial z}\frac{1}{p_o} = -\frac{2\pi}{L}\frac{\sinh\frac{2\pi}{L}(d-z)}{\cosh\frac{2\pi d}{L}} \qquad [3.2]$$

Improvements to Putnam's method incorporate a poro-elastic sea bed model. Despite the complication of the problem and the increased intricacy of the solution there are certain limiting cases, realistic in nature, where the final expressions are not significantly different. The relative compressibility and permeability of the material determine whether or not practical simplifications can be made to reduce the equations to simpler expressions. Yamamoto (1978) showed that for most soils the equation for excess pore-water pressures within an infinitely thick deposit beneath the sea-bed interface is:

$$\left|\frac{p}{p_o}\right| = e^{-\frac{2\pi z}{L}}. \qquad [3.3]$$

The vertical pressure gradient at the bed is:

$$\frac{1}{p_o}\frac{\partial p}{\partial z}\bigg|_{z=0} = -\frac{2\pi}{L}. \qquad [3.4]$$

The effective stresses, σ' (horizontal, vertical and shear) were also given in the solution. Although the stresses are all equal in magnitude, the shear stress is ninety degrees out of phase with the vertical and horizontal stresses.

$$\left|\sigma'_x\right| = \left|\sigma'_z\right| = \left|\tau_{xz}\right| = p_o \frac{2\pi z}{L} e^{-\frac{2\pi z}{L}} \qquad [3.5]$$

In shallow water, the vertical pressure gradient at the interface can be simplified to:

$$\left.\frac{\partial p}{\partial z}\right|_{z=0} = -\pi\rho g \frac{H}{L} \cos 2\pi\left(\frac{x}{L} - \frac{t}{T}\right), \qquad [3.6]$$

where T is the wave period.

The linear elastic properties of the pore fluid, soil matrix, and the hydraulic conductivity of the porous material were included in Yamamoto's solution. Notice that the equations for an infinitely thick porous layer do not include these properties. Yamamoto emphasizes that for some sea floor soils the wave-induced pressures within a deposit of finite-thickness are dependent on the permeability and stiffness of the bed material. Madsen (1978) used a similar procedure also using consolidation theory and developed very similar equations. Unlike Yamamoto, Madsen included the effect of hydraulic anisotropy, but only considered a permeable layer of finite thickness.

Equation [3.1] and [3.3] become approximately equivalent when the thickness of the porous layer is greater than half a wave length. The implication is that for practical purposes the porous layer may be considered infinitely thick when the wave length is less than twice the bed thickness. This finding is in agreement with Putnam's conclusion that the material below $0.3L$ has no appreciable effect on energy dissipation (Putnam, 1949). The ratio between the vertical pressure gradient at the interface calculated from Equation [3.2] and [3.4] is shown in Figure 3.2. The pressure gradient at the interface is less sensitive to the thickness of the bed and both equations give similar values for a deposit of any reasonable depth. For a relative depth of $\frac{d}{L} = 0.3$ the infinite thickness approximation is within five percent of the finite depth solution.

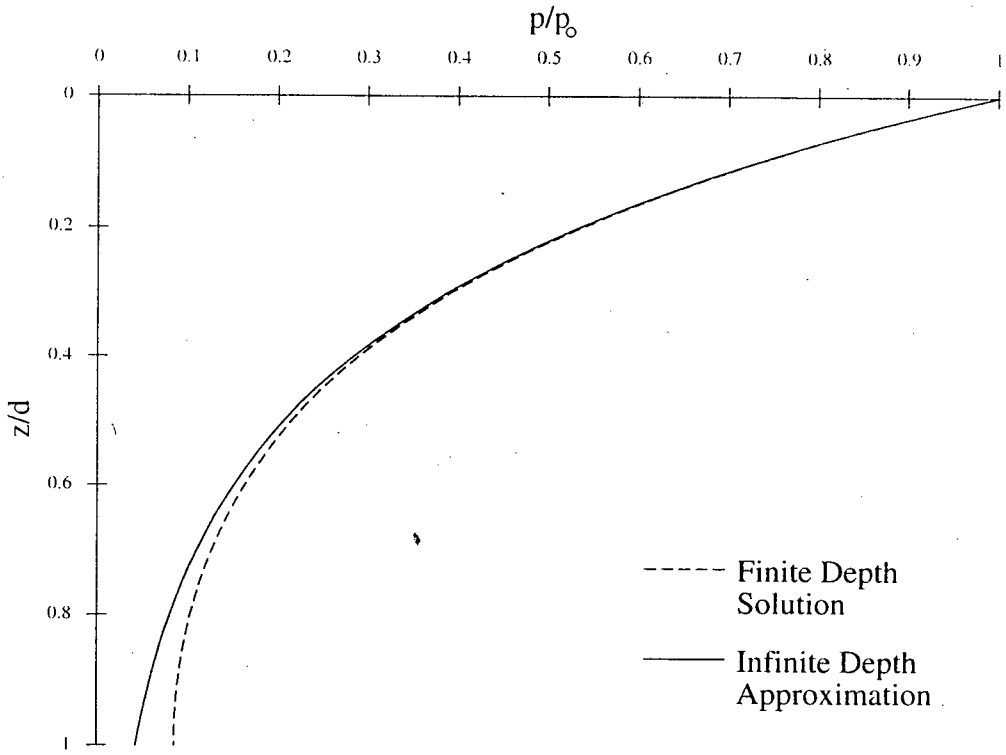

Figure 3.1 Comparison of Wave-induced Pore-water Pressure Calculations from Finite and Infinite Depth Solutions, $\frac{d}{L} = 0.5$

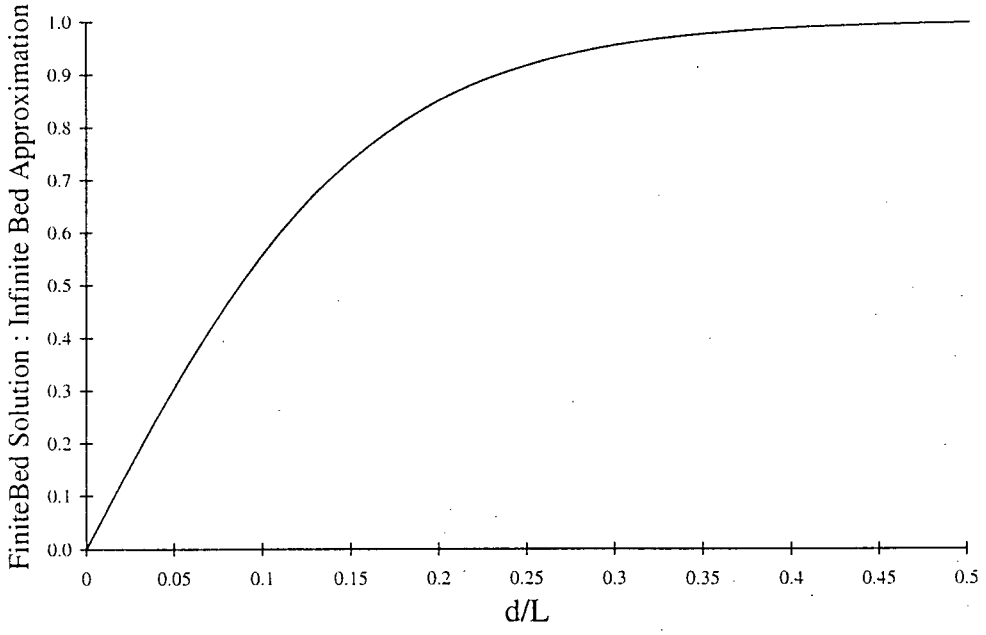

Figure 3.2 Ratio of Vertical Pressure Gradient at the Interface Calculated from the Finite Bed Solution and the Infinite Bed Approximation

3.2.2 Shallow Water and the Surf Zone

3.2.2.1 Solitary Waves Over Finite Depth Sea Beds

As waves propagate into shallow water, their form changes so that linear wave theory is no longer suitable to describe many of the properties and characteristics dominated by higher order effects. In deep water, Stokes higher order theories are known to perform extremely well; while cnoidal waves are more appropriate in shallow water. The solitary wave, the limiting case of a cnoidal wave in shallow water, has proved to be quite suitable when approximating long waves outside the breaker zone. This non-periodic, infinite length wave has also been used to simulate shoaling waves prior to breaking and has even been employed to model waves in the surf zone.

The pressure field in a porous deposit beneath a solitary wave has been solved by Peregrine and Packwood (1980). The velocity components within the porous deposit were also provided in the solution by differentiating the equation for pressure in both the x and y directions. The velocity components are directly proportional to the material permeability and are of particular interest to this study. Pressure gradients are a maximum at the bed surface and decay to zero below the interface.

Packwood and Peregrine treat both cases of a finite and infinite thickness deposits. Expressions derived for a layer of infinite thickness involve an infinite series, and are therefore much more cumbersome than the expressions proposed for a deposit of finite thickness that are much easier to use and provide much the same insight.

The vertical infiltration velocity beneath a solitary wave is:

$$\left.\frac{w_i}{K}\right|_{z=0} = -\frac{1}{\rho g}\frac{\partial p}{\partial z} = \frac{3}{2}\left(\frac{a}{h}\right)^2 \frac{d}{h}\sec h^2\sqrt{\frac{3}{4}\frac{a}{h}}\frac{x}{h}\cdot\left[2-3\sec h^2\sqrt{\frac{3}{4}\frac{a}{h}}\frac{x}{h}\right], \qquad [3.7]$$

where the subscript i denotes the infiltration velocity, and a is the wave amplitude. As shown in Figure 3.3, immediately beneath the solitary wave crest, the vertical infiltration velocity is a maximum and negative, that is into the porous bed. At some distance from the crest in both directions flow velocities are reversed and are out of the bed. The infiltration velocities reach a local maximum and decay to zero at the extremes.

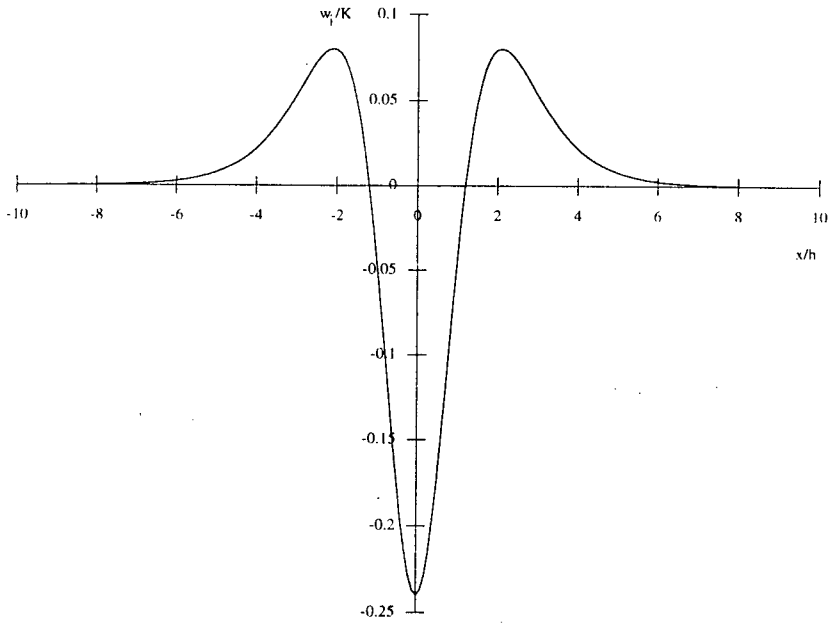

Figure 3.3 Solitary Wave: Vertical Component of Infiltration Velocity at the Bed, h=d, $\frac{a}{h} = 0.4$, after Packwood and Peregrine (1980)

The ratio of vertical to horizontal velocity at the interface can be shown to be:

$$\frac{w_i}{u_i} = \sqrt{\frac{3}{4}\frac{a}{h}}\frac{\left[2-3\sec h^2\left(\sqrt{\frac{3}{4}\frac{a}{h}}\frac{x}{h}\right)\right]}{\tanh\left(\sqrt{\frac{3}{4}\frac{a}{h}}\frac{x}{h}\right)}, \text{ for h=d.} \qquad [3.8]$$

This function is undefined at $x = 0$ which suggests that the flow in the porous bed is predominantly vertical beneath the crest. At the extremes, +∞ and -∞, the function asymptotes to the values of $\sqrt{3\frac{a}{h}}$, and $-\sqrt{3\frac{a}{h}}$ respectively. For large waves in shallow water, typical of storm attack, this suggests that the velocity components in the porous bed are again predominantly vertical. Assuming a breaker index of 0.7, the vertical infiltration velocity in the horizontal direction beyond five wave heights is nearly 1.5 times the horizontal infiltration velocity. Between the crest and tails of the solitary wave, there is a small region where the porous flow velocities are primarily horizontal at the interface.

3.2.2.2 Broken Waves and Bores Over Finite Depth Sea Beds

The form of shoaling shallow water waves is continually modified until the changes are so great to make the wave unstable. This instability, often associated with a critical wave steepness, causes the wave to break. The effects of wave breaking dominate the dynamics of the surf zone. To best predict the velocities and pressure gradients within the surf-zone, a suitable model should most probably represent a broken wave or bore.

Packwood and Peregrine also used the same approach that was used for a solitary wave to determine the velocity and pressure field beneath a bore. A hyperbola was used to simulate the pressure signature of a broken wave in the surf zone. The vertical component of the pressure gradient at the interface is:

$$\left.\frac{w_i}{K}\right|_{z=0} = -\left.\frac{1}{\rho g}\frac{\partial p}{\partial z}\right|_{z=0} = \frac{3}{4}\left(\frac{a}{h}\right)^2 \frac{d}{h} \cdot \tanh\sqrt{\frac{3}{4}\frac{a}{h}}\frac{x}{h} \cdot \sec h^2\sqrt{\frac{3}{4}\frac{a}{h}}\frac{x}{h}. \qquad [3.9]$$

Again the ratio between the vertical and horizontal velocities at the interface can be determined:

$$\frac{w_i}{u_i} = \sqrt{3\frac{a}{h}}\tanh\left(\sqrt{\frac{3}{4}\frac{a}{h}}\frac{x}{h}\right), \text{ for h=d.} \qquad [3.10]$$

In this instance, at $x = 0$ the function is equal to zero - indicating that vertical velocities will be dominated by the horizontal fluid movements at the interface. The above expressions reach maximum values of $\sqrt{3\frac{a}{h}}$ and $-\sqrt{3\frac{a}{h}}$ at $+\infty$, and $-\infty$. Predictions of vertically dominated flow at the interface may not be justified except for very large waves in shallow water.

In both instances, solitary waves and bores, Packwood and Peregrine (1980) show that wave damping from a deep coarse deposit can be greater than frictional damping in the bottom boundary layer. A similar conclusion was made more than thirty years earlier by Putnam (1949).

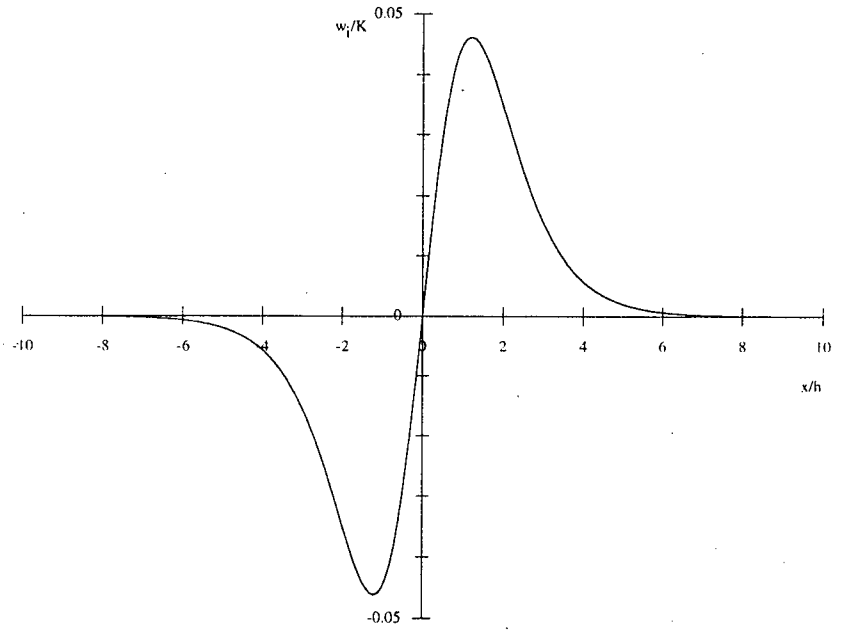

Figure 3.4 Bore: Vertical Component of Infiltration Velocity at the Bed h=d, $\frac{a}{h} = 0.4$, after Packwood and Peregrine (1980)

3.2.3 Seepage, Effective Stress, Liquefaction and Uplift

Another sea bed effect that can have a tremendous influence on sediment transport and incipient motion of individual grains is the forces associated with wave-induced pressures. Though the effects associated with hydrostatic pressure forces are minor; the effect of pressure gradients from excess pore-water pressures on bed material can be considerable. It is well known that large hydraulic gradients give rise to what is commonly called a seepage force. If the gradient exceeds a critical value then uplift and instability occurs. Similarly, liquefaction occurs if excess pore-water pressures exceed the vertical stress acting on a soil mass. Both these conditions are serious from a geotechnical or sediment transport perspective since the material no longer provides any frictional resistance. Wave-induced pressure gradients can also exert forces on particles that rival gravity, and effectively augment buoyancy generated by the hydrostatic pressure gradient. Large enough pressure waves exert a buoyancy force capable of inducing sand liquefaction. Exfiltration from the bed can also generate additional buoyancy forces that affect incipient motion and enhance sediment entrainment and suspension.

The pressure gradient at the bed is largely dependent on wavelength, but the work of Mei and Foda (1981) and Moshagen and Torum (1975) also indicate a minor dependence on hydraulic conductivity that increases with decreasing permeability. This effect is shown in Figure 3.5. The implication is that fine sands may be more easily liquefied than fast draining coarse sands.

The general equation for pressure given by Mei and Foda (1981) can be differentiated with respect to z in order to give the vertical pressure gradient at the interface.

$$\frac{\partial p}{\partial z}\Big|_{z=0} = -\frac{p_o}{1+m}\left[\frac{2\pi}{L}+\frac{m}{\sqrt{2}\delta}\right]\cos 2\pi\left(\frac{x}{L}-\frac{t}{T}\right) - p_o\frac{m}{1+m}\sin 2\pi\left(\frac{x}{L}-\frac{t}{T}\right)\frac{1}{\sqrt{2}\delta} \qquad [3.11]$$

The stiffness ratio is given by m, and the boundary layer thickness, δ, is shown to be proportional to the hydraulic conductivity.

$$\delta = \sqrt{\frac{K}{\rho g}\frac{T}{2\pi}}\left[\frac{n}{\beta} + \frac{1}{G}\frac{1-2\nu}{2(1-\upsilon)}\right]^{-\frac{1}{2}} \qquad [3.12]$$

β is the bulk modulus of the fluid; G is the shear modulus of the solid matrix; n the void ratio, and υ Poisson's Ratio. Mei and Foda assumed a poro-elastic soil matrix, but also considered the pore fluid to be compressible. Air entrainment in the pore fluid drastically changes the sea bed response.

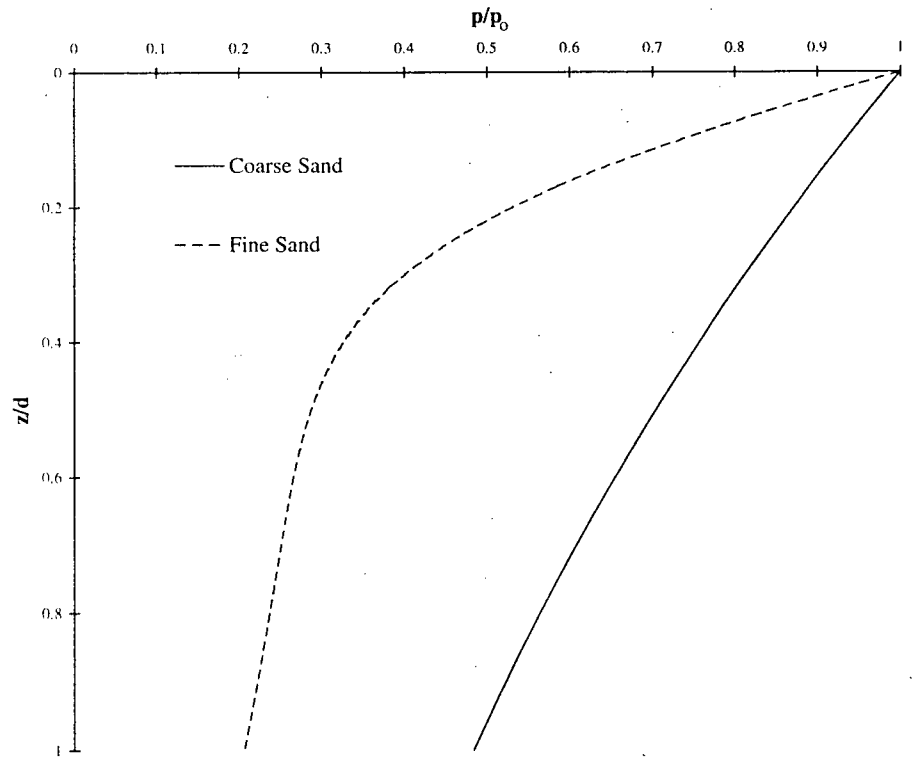

Figure 3.5 Effect of Bed Permeability on Pore Pressure, after Mei and Foda (1981) Coarse Sand ($K=10^{-2}$ ms^{-1}), and Fine Sand ($K=10^{-4}$ ms^{-1}), $n=\frac{1}{3}$, $\upsilon=\frac{1}{3}$, $G=10^8$ N/m^2, $\beta=10^8$ N/m^2, L=71 m, T = 8 s, d = 10 m, h = 10 m

For an isotropic, infinitely thick deposit, Moshagen and Torum (1975) proposed the following expression for the pressure gradient at the interface:

$$\left|\frac{\partial p}{\partial z}\right|_{z=0} = -p_o\left[\left(\frac{2\pi}{L}\right)^4 + \left(\frac{2\pi}{T}\frac{n\rho g}{K\beta}\right)^2\right]^{\frac{1}{4}}. \qquad [3.13]$$

The approach assumed the water to be compressible and the soil matrix to be incompressible. These conditions are not common in fully saturated deposits. Consequently, predictions are unrealistic and do not agree well with filed observations (Finn et al, 1983). Ignoring material properties, Equations [3.11] and [3.13] can be reduced to Equation [3.3].

3.3 Time Averaged Flow Field and Set-up Induced Percolation

The cyclic nature of transient pore-water pressures may reduce their net effect or even nullify their action when averaged over many wave cycles. The effects from time averaged residual pressure gradients, enduring and building over time, may be more far-reaching. Longuet-Higgins (1983) has shown that the time averaged onshore pressure gradient produces a circulation of water within a porous beach. The theoretical model assumes the flow to obey Darcy's Law, and ignores the set-down outside the break point.

$$\mathbf{q} = -\frac{K}{\rho g}\nabla\overline{p} = \nabla\phi \qquad [2.10]$$

The shoreward pressure gradient, constant in the surf zone from break-line to the run-up point, generates a fluid potential that drives the sweeping flow of pore fluid. Longuet-Higgins (1983) solved the Laplace equation in an elliptical coordinate system to give a simple expression for the fluid potential.

$$\phi = C \cdot l \cdot e^{-\xi} \cos\eta \qquad [3.14]$$

$$0 \le \xi \le \infty, 0 \le \eta \le \pi$$

C is a constant proportional to the material permeability; l is half the length of surf zone from break-point to maximum run-up, and ξ and η are the elliptical coordinates.

For two dimensional flow there exists a conjugate stream function constant along the streamlines.

$$\psi = C \cdot l \cdot e^{-\xi} \sin\eta \qquad [3.15]$$

Streamlines trace the flow field within a porous beach. It is apparent from Figure 3.5 that the zone of influence extends landward, far beyond the run-up point, and well into the beach itself. Infiltration from the upper beach circulates deep beneath the surface and returns outside the break point. For steady flow, streamlines, pathlines and streaklines are identical. These lines are revealed when dye is injected into a porous laboratory beach and confirm the theoretical predictions by experiment.

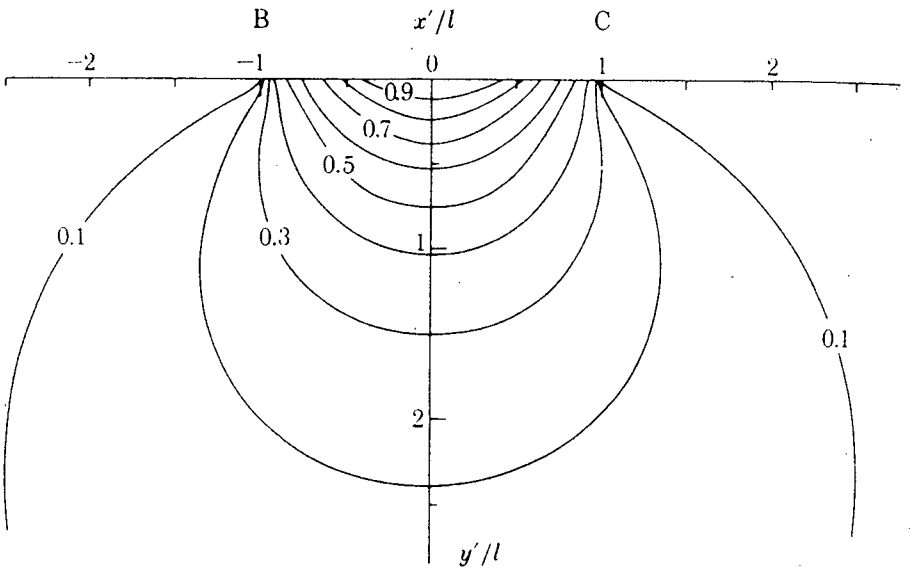

Figure 3.6 Streamlines Within a Porous Beach, Longuet-Higgins (1983)

Chapter 4

Run-up, Uprush and Backrush, and Extreme Velocities and Surface Elevations

4.1 Experimental

The erosive capacity of wave attack is determined by the power of the uprush and the strength of the backrush. Run-up levels establish the maximum amount of potential energy that can be transferred to the return flow and converted into backwash velocity. Run-up, defined as the point of maximum elevation reached by the uprush above the still-water level, dictates the height above the water surface that shore-protection works must be built to provide sufficient freeboard. Overtopping often leads to widespread crest damage or even failure of both conventional and rubble mound breakwaters. Similarly, protective berms on beaches maintain foreshore stability from elevated run-up levels and safeguard against erosion.

Run-up and uprush strength are reduced by loss of water into the bed; while reduced backwash by infiltration provides less resistance to incoming waves and allows stronger uprush. The flow depth and velocity are diminished as a surge propagates over a permeable bed. The infiltration of water under a surging bore reduces the volume of the backwash and its capacity to transport sediment offshore. The transfer of water into the beach and the nullification of its forward thrust results in the exchange of momentum between the infiltrating water and the beach face.

Granthem (1953) was one the first to study the effect of porosity (more accurately permeability) on run-up levels for sloping structures. His experiments were confined to a fixed bed but did test three model conditions: a smooth impermeable surface, a structure made of 1½ inch angular stone (n=0.326), and a slope composed of ¼ inch pea gravel (n=0.289). Run-up levels were recorded for varying wave steepness and different slope angles. Granthem recognized the advantage of structures with high relative roughness and large porosity and appreciated the additional freeboard requirements to prevent overtopping on smooth surfaces.

Savage (1958) extended Granthem's work to include a wider range of slopes from 1:30 to vertical. Savage also included permeability measurements and particle gradations as further improvements. The materials used by Savage ranged from a fine sand (D_{50} = 0.2 millimeters, K = 0.0003 ms^{-1}) to gravel (D_{50} = 10 millimeters, K = 0.13 ms^{-1}). Results show that material permeability had a major effect. Relative run-up on porous slopes were consistently and considerably less than values recorded on smooth slopes. Additional reductions in run-up levels were observed for slopes composed entirely of the test material compared to surfaces roughened with a thin layer of the same material. The effect of slope permeability was more pronounced than the effect of slope roughness. Savage also reported small but significant run-up reductions on a slope composed entirely of 10 millimeter material compared to a slope with only a 5 inch layer over a smooth bottom. Run-up levels on permeable slopes rapidly diverged from smooth slope values as the structure flattened and lengthened The elongated structure dissipated more energy and had greater infiltration capacity. Run-up on permeable structures was more sensitive to the slope angle than were smooth slopes; especially at steep angles.

Wave breaking and reflected wave energy were noticeably affected by the angle of the structure. Savage noted the breaker type depended on the behaviour and timing of the backwash.

Run-up on permeable slopes was shown to decrease as wave steepness increased. Increased wave steepness is known to increase wave breaking and energy dissipation through breaking.

4.2 Numerical Simulations

Van Gent (1994) described the results from a numerical model that coupled a hydraulic model and a porous flow model. The hydraulic model used equations similar to those found in Section 2.1; while the porous flow model used an extended Forchheimer equation. Although the numerical model was intended for the simulation of wave action on and in coastal structures such as berm breakwaters and submerged breakwaters, comparisons made between permeable and impermeable structures should also apply to beaches. Conceivably, findings from these simulations should be similar for permeable and impermeable beaches, though perhaps to a lesser extent. Van Gent (1994) reported much greater run-up levels and larger extreme surface elevations at breaking for an impermeable structure compared to a permeable structure. Extreme backrush velocities on an impermeable breakwater were as much as double or triple those reported for permeable structures without a core. This effect applies to beaches and explains why impermeable beaches show much more seaward transport of sediment. Simulations on a permeable structure with an impermeable core were also included.

The contrast between the results from a simulation on an impermeable structure and results from a porous structure without a core emphasized the influence of the subsurface region on the flow field. We are also reminded as to the purpose of a permeable layer at the surface. van Gent also showed the results from flow field visualizations that added a qualitative impression of the internal region within permeable structures and confirmed previous understandings.

Packwood (1983) found that run-up of a single bore on a plane, gently sloping beach was very little influenced by permeability. Simulations from a numerical model showed that the influence of the bed was much more apparent in the backwash. Packwood used a similar long wave hydraulic model including unsteady Chezy bed friction to simulate the run-up of a bore on an impermeable and permeable beach ($K = 10^{-3} ms^{-1}$). Friction greatly reduced run-up levels, although numerical predictions were much greater than measured values. The model treated porous flow within the beach to be purely vertical. This assumption was unrealistic but was a reasonable simplification to investigate the effect of a single bore before lateral flow from multiple wave cycles affected pore-pressures.

Packwood noted that the influence of beach porosity on wave motion in the surf zone was twofold. A porous beach attenuates incoming waves, and the unsaturated bed soaks up water from the run-up and back-wash. Water lost into the beach caused the weakening of the backrush which Packwood argued would increase the amount of material deposited at the maximum run-up point. Uprush and backrush on a saturated beach were stronger. Stronger backwash in conjunction with seepage forces from water flowing out of the beach can increase net offshore transport of material.

Chapter 5

Beach Stabilization Using Drain Systems

Increased infiltration promotes beach stability and contributes to accretion. This effect is crucial to the success of a new "soft" shore protection system known as Beach Management. Drains buried beneath the beach face control the water table within the beach and artificially increase infiltration. This effect has been reported in the field and studied in laboratory. Beach face pumping is an attractive alternative to "hard" conventional shore protection structures and it enables selective operation which provides protection when the system is more effective, most economical and most required.

5.1 Laboratory Studies

Care must be taken when interpreting results from model tests and caution should be exercised when scaling findings to prototype. The problem of cross-shore transport on a permeable beach by wave action is especially dangerous since it involves the interaction of three processes that probably do not scale to prototype correctly. The three elements are the wave hydrodynamics, sediment transport and percolation. Nevertheless, laboratory experiments and model studies are often the source for most of the understanding and insight for problems that researchers are unable to model numerically because of insufficient understanding or excessive complexity.

Weisman et al report that Froude models that scale sediment size by the fall velocity criteria do not scale permeability properly. They argue that hydraulic models that aim to

reproduce percolation processes will be less effective than prototype systems because of this scale effect. Wave and sediment dynamics are preserved, but infiltration effects are not because of the conflicting requirements for the particle size of the model sediment. Model beaches are not only wetted more frequently because of the reduced wave period, but they drain more slowly because of the reduced particle size required to preserve similitude between model and prototype suspended sediment motion.

Little work has been done on beach stabilization and erosion control using pumped drains. The work of Ogden and Weisman (1991) contains a comprehensive review and summary of most known publications from field and laboratory studies. A better presentation of their original work on drain position and the influence of tides is found in Weisman et al (1995). The set-up used by Ogden and Weisman used perforated pipes beneath the beach face that drained by gravity into a sump. The system generated smaller flow rates than infiltration induced by suction. The flow rate from the system increased with larger waves and also as the depth of the intake below still water was increased. The beach drain proved to be effective for a wide range of wave heights and Weisman et al recommended continuous operation of Beach Management Systems based on this result. Pumped profiles were steeper and showed the building of a large onshore berm.

Cited as the first engineering investigation into the effect of a sub-sand filtering system, Machemehl et al (1975) reported accelerated accretion and increased onshore sediment movement in the fore-shore region under very high pumping rates. The sub-sand filter controlled the seaward movement of sediment and encouraged accretion that lead to the formation and enlargement of the onshore berm which initiated shoreline advance.

Kawata and Tsuchiya (1986) used regular and solitary waves and observed the disappearance of ripples while pumping and commented on the obvious reduction in bottom roughness. They stated the swash movement of sediment up and down the beach face was be largely controlled by the permeability of the beach. Kawata and Tsuchiya also commented that longshore sediment transport would be reduced during pumping.

All investigators reported reduced flow rates and poorer pumping efficiency as material accumulated onshore and further covered the buried intake. Diminished sediment activity and increased grain stability in the offshore zone were caused by a higher threshold of motion which was apparently due to the increased drag on particles and reduced turbulence from pumping.

Unpumped sections were scoured because their sediment supply was redirected onshore by the beach management system. This condition is similar to clear-water scour of piles and piers.

5.2 Field Studies

5.2.1 Early Research

Chappell et al (1979) described two field experiments where beach watertables were regulated by pumping wells. Results strongly suggested that the steepening of the beach and aggradation from suspended sand deposited on the beach face was induced by artificially lowering the watertable and reducing the backwash in the affected area. These effects were not observed for the rest of the beach outside the growth zone. Coarse, platy shells one or two millimeters in diameter were also deposited in the zone of influence. A thin mat was deposited

in front of the 35 meter long well-line and extended 10 meters seaward. Marked aggradation in the middle of the growth zone was on average seven centimeters thick. The accretion occurred even while competing with longshore currents. Dye tracers did not indicate that the accretion was the result of a sand promontory opposite a rip.

Pumping was also thought to reduce front failure, slumping and liquefaction on eroding beaches. Chappell et al commented that although the magnitude of the swash induced pressure wave was unaffected by pumping, the liquefaction threshold was reduced. Water level pulses were detected in observation wells although the damped surges lagged each wave breaking event. Chappell et al also included rough calculations on the ratio of the incoming wave energy flux and the energy expended by pumping. The pump discharge was determined to be 1.5 % of the swash flux onto the beach. Based on these rough calculations, Chappell et al reported that long-term operation of a permanent facility would not be costly.

5.2.2 Permanent Installations

Beach-face pumping as a permanent method of shore protection has been in use on the coastline of Florida since 1988 and Denmark's North Sea Coast since as early as 1983. The beach management system, still in its infancy, promises to be a reliable and effective method of erosion control and shore protection. All four sites report excellent performance throughout all stages of their operation: immediately following installation, during destructive winter storms and especially when calm weather conditions prevail. The Beach Management System is reported to stabilize eroding beaches and initiate accretion with negligible impact on the environment. Considerable accretion and steepening of the beach were reported in the affected

areas. Filtered sea water pumped from the beach can be used for heat exchangers, salt water marshes, sea-water swimming pools or simply returned to the ocean.

Surveys indicate that unpumped sections adjacent to the test sections were influenced by the drain pumping and beaches downdrift were reported to benefit from excess material supplied from the sand bulge. Promotional material also claims that the pumping does not block the longshore drift. The ability to stabilize beach material and restore shorelines ravaged by periodic winter storms make the Beach Management System ideal to be used in conjunction with artificial nourishment programs.

Some restrictions apart from limitations on the wave climate increase the likelihood of success. Ideally, the beach material should be a medium sand. Fine material, especially silt, make dewatering difficult; while coarse gravel needs much more infiltration and requires uneconomical flow rates. Milder beach slopes are also desirable. It is also important to have a sufficient beach thickness to provide enough cover for the drains during storm activity and to protect against breaker induced scour. Site specific geotechnical investigations are practically essential. It has been suggested that beaches with active suspended sediment transport are more suitable for this method of shore protection. It has also been proposed that the system is more effective for longer period waves which allow more time for the advancing waves to percolate into a permeable beach.

5.2.2.1 Denmark

5.2.2.1.1 Hirtshals West

The effect of beach face pumping was discovered by accident at Hirtshals, Denmark in 1981 when the Danish Geotechnical Institute installed a horizontal slotted PVC pipe and gravel filter below a well-sorted medium sized sand beach to supply large quantities of filtered sea water that were required for heat pump systems. Winter erosion did not occur. Instead, the beach grew wider when pumped during the winter storm season. The shoreline was reported to have moved 20 to 30 meters offshore and the pump discharge was substantially reduced. Excess sand was used to nourish a neighbouring beach and dry fine grained sand was blown onto nearby streets. The local council still tender offers to have twenty-five thousand cubic meters of sand removed to nourish other beaches.

5.2.2.1.2 Hirtshals East

The beach drain was tested at a second location to determine its applicability and efficiency under poor site conditions. The beach at Hirtshals East was composed of much finer material that contained some silt and clay. Effects similar to those at the western site were reported despite unfavourable soil conditions. Accretion preserved or even extended the shoreline seaward despite forecasts based on historical records that predicted erosion of the beach. Erosion and damage from a storm that occurred during construction before the system was operational was reported to have been restored within two months of activating the Beach Management System.

5.2.2.1.3 Thorsminde

Hansen (1986) described a full scale test at Thorsminditangen, Denmark. The beach was located on the open ocean and was frequently ravaged by intense North Sea storms which were responsible for coastal erosion of 3.9 meters per year. With the drain system in operation, erosion was halted and the shoreline stabilized and moved 10 meters out from its original position. Pronounced accretion downdrift of the drain illustrated the effective zone of influence extended beyond the drain limits and illustrated the potential for adjacent sections to benefit from increased onshore sediment movement.

Considerable erosion accompanied intentional shut-off and the attack of the one hundred year storm. Reactivating the drain system restored the coast to its original position within a year.

The test of the coastal drain system was intended to reproduce the effect observed under less severe weather conditions at Hirtshals in North Jutland, Denmark. Full scale tests at Thorsminditangen stabilized the shoreline twenty to twenty-five meters from the drain line with little environmental impact and more economically than ordinarily possible through beach nourishment.

5.2.2.2 Sailfish Point, Florida

The first commercial application of the beach drain system was built in 1988 at Sailfish Point on Hutchinson Island located on the open Atlantic Ocean near Stuart, Florida. Documented erosion of 135 feet plagued the coast over a ten year period. A geotechnical investigation determined that the site was suitable for beach face pumping. The median grain size was 0.3 millimeters, and the permeability was estimated to be 0.0003 m/s. This setup

included an improved design and a more advanced intake system. Pumping rates were affected by the tidal conditions and varied between 150 and 400 cubic meters per hour. Moderate accretion and stability in the protected zone were reported while control sections continued to erode.

5.2.3 Geosynthetics and Gravity Drainage

A low-cost gravity drainage system using geosynthetic strip drains was reported by Davis et al (1992). An array of "shore-normal" strip drains 25 meters in length were buried 5 to 15 meters apart in a beach composed of a sand 0.5 millimeters in diameter. A well within the beach monitored the level of the watertable. The drained beach profile not only showed a lower watertable level but also exhibited noticeable steepening. The tidal response was also affected. Drained sections showed increased accretion in calm weather and increased stability.

Chapter 6

Experimental Investigation

6.1 Experimental Set-up

An experimental investigation was conducted to determine the effect of infiltration on the equilibrium beach and to what extent the exchange of fluid between the internal and external regions controls cross-shore movement. The role of infiltration in controlling the beach slope was illustrated in two different ways. One experiment involved the use of sand mixtures with different gradations to investigate the effect of changing the bed permeability; while another used a pumped drain system under the beach to artificially induce infiltration. Experiments studying the effect of changing bed permeability were conducted in the main wave flume; while the tests that investigated the effect of beach-face pumping were performed in a smaller flume. The equilibrium profiles were analyzed to compare the stable beach slope for different infiltration conditions.

6.2 Main Wave Flume: Permeability and Sediment Gradations

The tests were performed in the wave flume of the Hydraulics Laboratory of the Department of Civil Engineering at the University of British Columbia. The flume, shown in Figure 6.1, is 25 meters long, 0.62 meters wide and 0.75 meters deep. All tests were run with a water depth of 0.5 meters. As Figure 6.1 indicates, a false bottom, inclined at 4 degrees(1:15), lay beneath the beach. A six meter long beach was constructed at the far end of the wave flume

on top of this false bottom. The toe of the beach rose from the bottom of the flume to the full flume depth of 0.75 meters. An initial slope of 8 degrees (1:7) was used for the majority of the experiments. The bed was made as thick as possible to reduce the effect of impermeable boundaries on the complete development of the flow field. Each material was tested separately and subjected to the attack of storm waves simulated by a series of plunging breakers. The computer-generated monochromatic wave had a period of 2.0 seconds, and the calculated wavelength from the dispersion relation is 4.06 m. Waves propagated through transitional water $\left(\frac{d}{L} \approx \frac{1}{8}\right)$ where they shoaled and broke over a deep mobile bed. Wave heights and intermediate profiles were recorded hourly until the beach reached a stable equilibrium. Pore-water pressures were also recorded in some tests. Profiles were recorded using an electronic bed profiler connected to a VAX3200 work station. Measurements of wave reflection were done with an array of three capacitance-type wave probes and the program REFLM to analyze the record.

Different sediment gradations were created from the combination of two specially selected types of high quality sand purchased from a local supplier. A clean, uniform 3 millimeter sand made up the coarse fraction. Ninety-eight percent of this material was retained between the 2 millimeter and the 4.75 millimeter sieves; while only one percent of the material was larger than the 4.75 millimeter sieve. The fine component of the gradations consisted of a 0.3 millimeter sand with less than one percent passing the 75 micron sieve. Fifty percent of the fine material was retained between the 0.246 millimeter and the 0.417 millimeter sieves. These materials were combined in exact proportions to produce five unique blends with distinct hydraulic properties. Materials were thoroughly mixed in a cement mixer before being placed in the flume to ensure that the bed was isotropic throughout and the hydraulic conductivity was uniform. Particle size distributions are shown in Figure 6.2

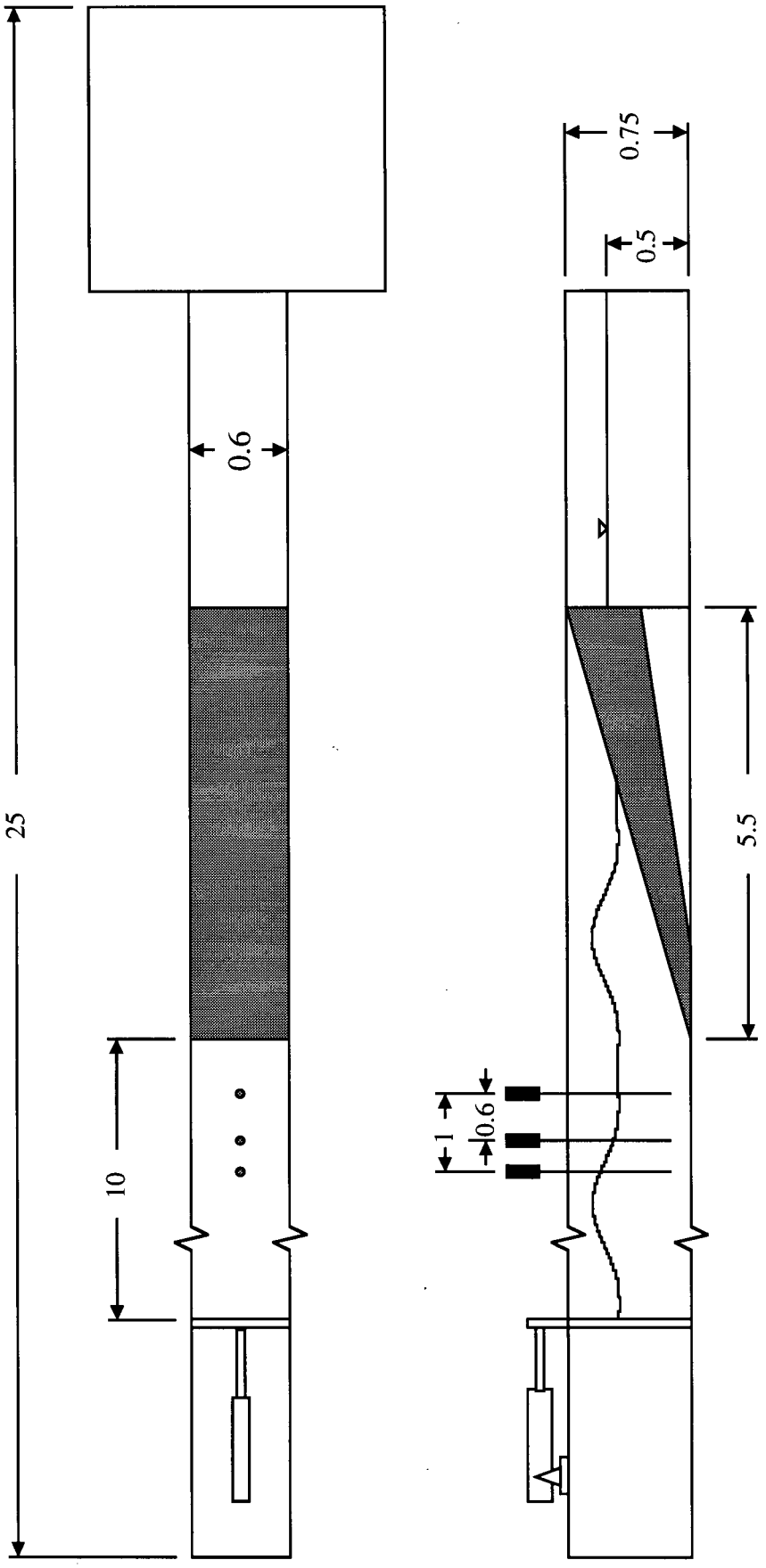

(all dimensions in meters)

Figure 6.1 Main Wave Flume

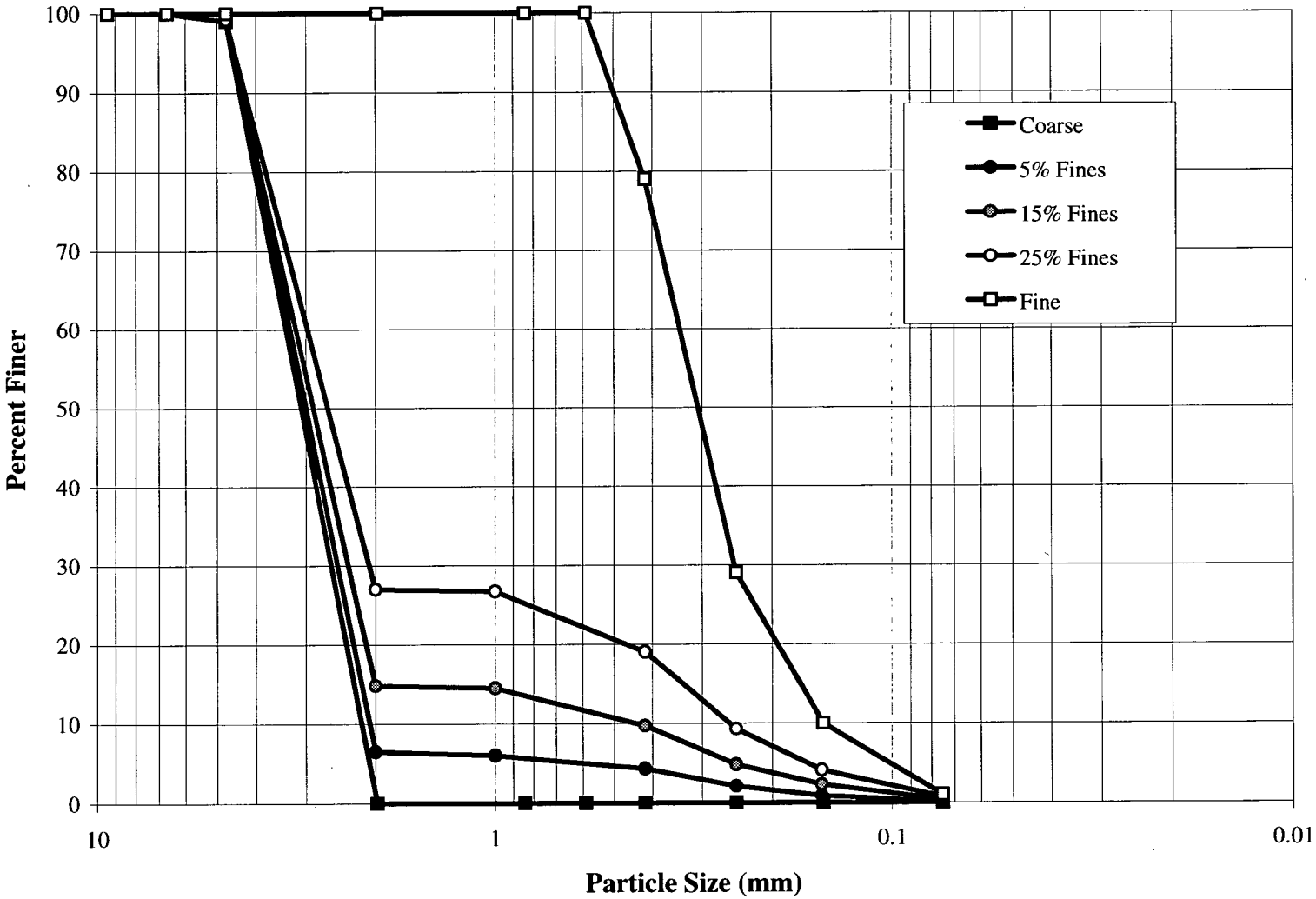

Figure 6.2 Particle Size Distributions

A comparison between hydraulic conductivity predictions using the empirical equations of Hazen (1911) and Krumbein and Monk (1942) are shown in Table 6.1.

	Hydraulic Conductivity K (ms^{-1})	
Material	Krumbein and Monk	Hazen
0 % Fines	4.9×10^{-2}	5.1×10^{-2}
5 % Fines	4.4×10^{-2}	4.4×10^{-2}
15 % Fines	3.7×10^{-2}	2×10^{-3}
25 % Fines	6.1×10^{-3}	6.7×10^{-4}

Table 6.1 Permeability Predictions

6.2.1 Wave Flume and Wave Generator

The computer controlled wave generator was a servo-driven, linear-actuator capable of both monochromatic and random wave generation. Random waves, although a more realistic representation of a natural sea-state, were not used in this study. Regular (monochromatic) waves were used to ensure better reproducibility of results and to ensure that the location of wave breaking was stable and that surf zone dynamics were consistent from one wave cycle to the next. Drive signals were computed on a VAX3200 work station equipped with GEDAP, GPLOT and a RTC software.

6.2.2 Instrumentation

6.2.2.1 Bed Profiler

The profiler was designed and constructed for this thesis to automatically record the beach profile and was based on the simple rotating arm type used at laboratories such as the National Research Council and Queen's University. A three-wheeled carriage mounted on rails traversed the length of the beach while an optical encoder coupled to the axle recorded the horizontal position from the baseline. A lightweight wheel contacted the beach face and tracked its position. The wheel was connected to a 1 meter long arm that was free to rotate through a vertical plane. The rod was coupled to a calibrated three-quarter-turn potentiometer that recorded the arm's angular displacement from the horizontal. A FORTRAN program, also written as a part of this work, calculated the vertical and horizontal coordinates of the beach profile. The profile position was recorded every 1.6 millimeters that the carriage traveled. This was the maximum resolution of the optical encoder. As a result, most profile records contained four thousand data points to describe a beach approximately six meters long.

6.2.2.2 Wave Probes and Reflection Measurement

Water surface elevations were recorded hourly throughout each test. Capacitance-type wave probes were used. These devices were extremely precise and highly linear.

Two different arrangements were used for two different purposes. The first set-up was primarily intended to record the time series of wave action at two characteristic locations; one in the uniform deepwater section; and one in the surf zone inside the break point. This arrangement

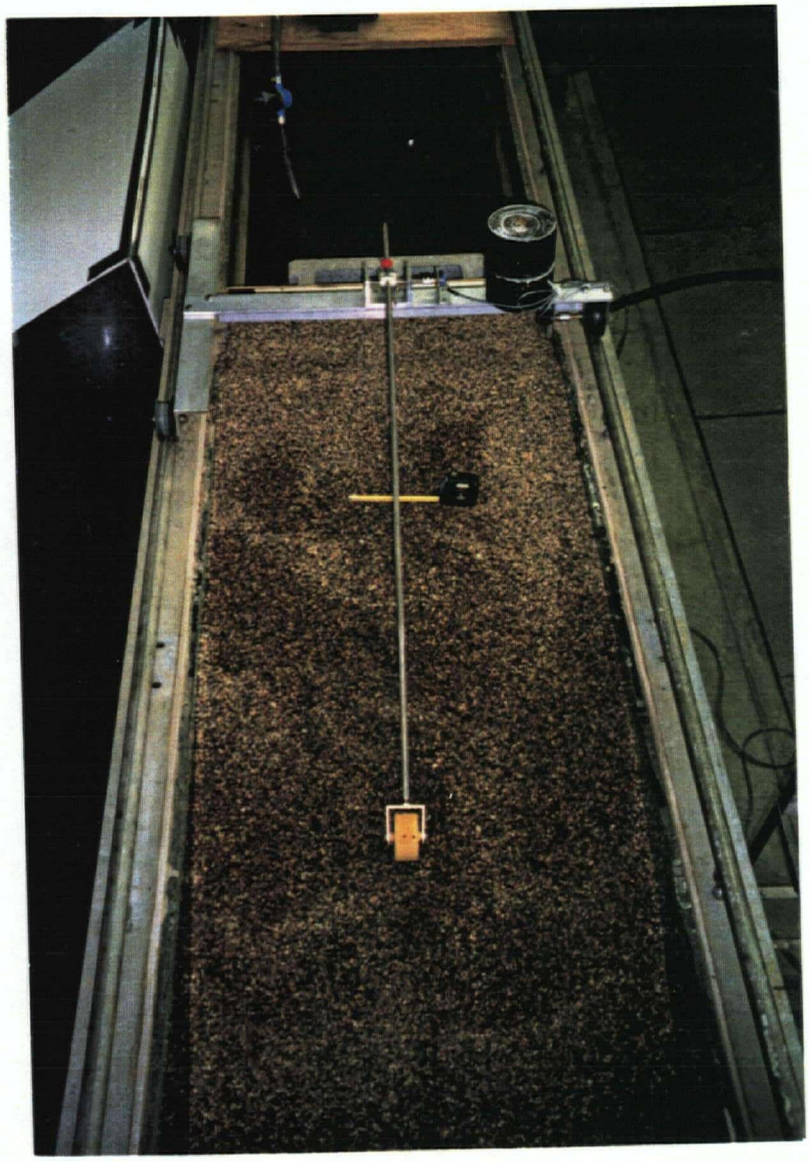

Figure 6.3 Bed Profiler

used only two gauges and was only used as a qualitative means of evaluating the effects of wave reflection. Offsets were taken before each test to ensure that the still water level corresponded to zero elevation on the probe. This way, any lowering of the mean water surface was recorded. The five minute time-series was analyzed using GEDAP software to determine the wave properties and to perform any statistical analysis.

The second configuration was used to measure wave reflection and determine the characteristics of the incident and reflected waves. This set-up was used when wave records from the two-probe configuration (described above) indicated that wave reflection wave significant. Three probes were mounted in a line parallel to the direction of wave propagation midway along the length of the flume where the water depth was uniform. Probe spacing was selected based on the recommendations of Mansard and Funke (1980) and so that the wave height error associated with this method was minimal (see Isaacson, 1991). The selected spacing was 0.4 meters (one tenth the wavelength) between the first and second probe, and 1.0 meter (one quarter the wavelength) between the first and third probe. Using the analysis procedure described in Mansard and Funke (1980) and the GEDAP program REFLM, the incident and reflected wave heights were obtained from a 100 second wave record. The coefficient of wave reflection was also recorded.

6.2.2.3 Pressure Transducers

Sensotec model LJS silicon diaphragm pressure transducers rated up to 1 psi were selected to measure pore-water pressures. Offsets were taken prior to starting each test so that the transducers recorded pressures above hydrostatic. This model has 0.25% accuracy and 4 times overpressure rating. The pressure port was equipped with a porous disc attachment to

prevent sand from damaging the pressure diaphragm. This "snubber" also ensured that the transducer was measuring the pore-water pressure and not the total pressure of the surrounding soil. Pacific Model 8255 amplifiers were used to amplify the low voltage signal and filter out the high frequency noise. Transducers were sampled at 20 Hz but were filtered at 10 Hz to avoid any alias. Williamson and Hall (1992) have shown 20 Hz to be a satisfactory frequency to measure external wave pressures on a rubblemound breakwater.

This system proved to be reliable and highly linear over 95% of the transducer range. One problem observed with this type of transducer was that the signal was observed to "drift". This phenomenon made it difficult to record the time averaged set-up pressures, but the magnitude of the pressure disturbance generated by individual waves was recorded with sufficient accuracy. A time series record of such an event is shown in Figure 6.5.

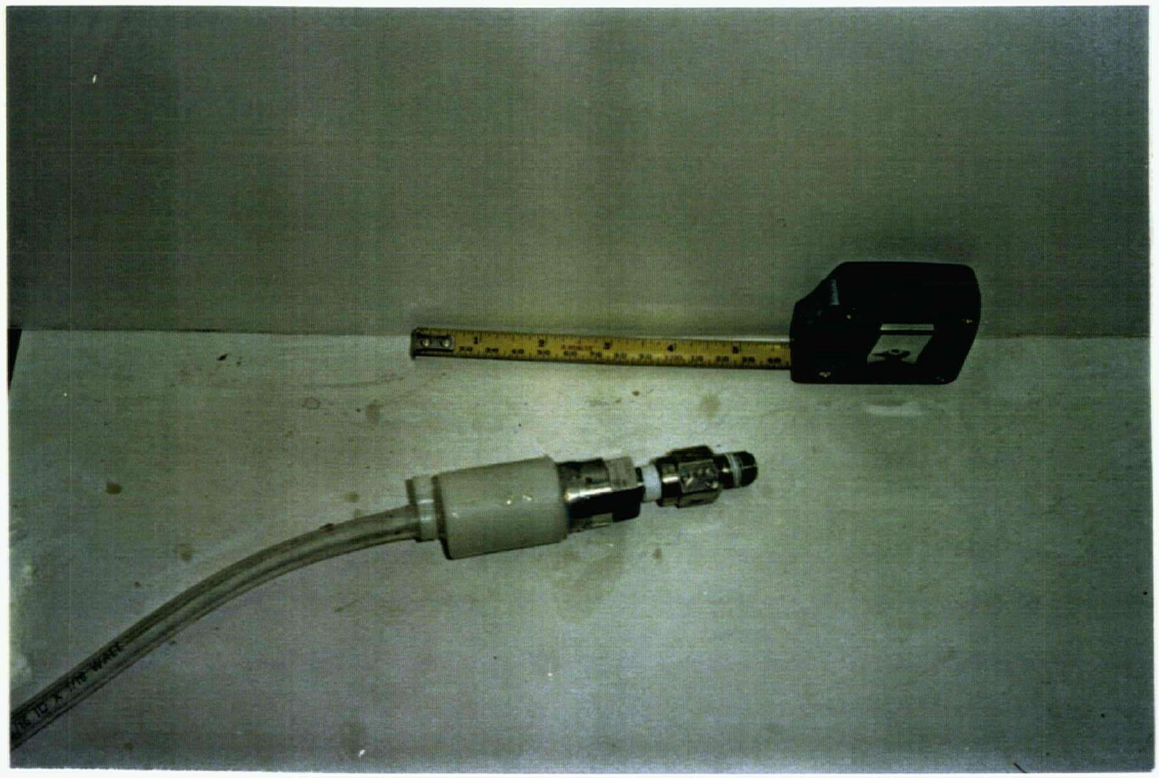

Figure 6.4 Pressure Transducer

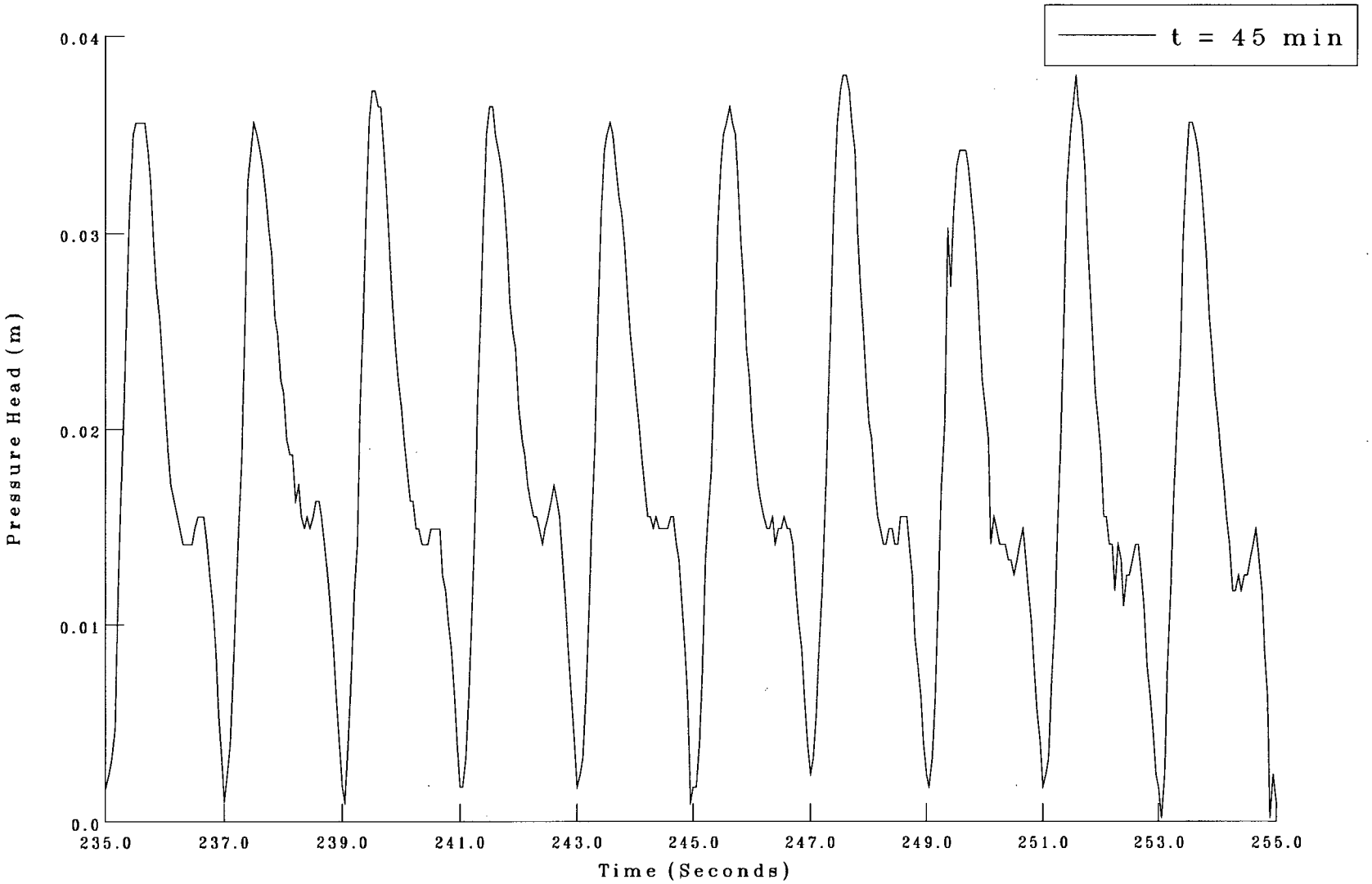

Figure 6.6 Time Series Record from a Pressure Transducer Buried Beneath the Beach Face Within the Surf Zone

6.3 Small Flume: Pumping Induced Infiltration

These tests were performed in the small flume shown in Figure 6.6. These preliminary tests were carried out in the small wave flume to examine the response of a beach to pumping. Being on a small scale, these experiments were much easier to carry out than in the large flume and this allowed easier testing of a range of conditions. Although this flume is smaller, notice that it has an overflow behind the wave paddle that was essential to control the water level during pumping. The head tank behind the sand beach was also maintained at a constant elevation. A plunging breaker was generated to simulate the destructive power of a storm event. A mobile-bed hydraulic model was constructed to study the complicated surf zone processes. The bed was made as thick as possible to minimize the effect of impermeable boundaries and obstructions on the complete development of the natural flow field. Again, a deep, uniform sand beach was constructed at the far end of the flume, a distance of about 3.5 meters from the wave paddle. Suction to the bed was supplied by a 10 USGPM self priming pump capable of generating 3.3 meters of net positive suction head. The suction was distributed through a manifold to a 30 centimeter long container of three quarter inch gravel installed within the beach and spanning the width of the flume. The top of the container was covered with a non-woven geotextile to prevent the migration of fine beach material through the granular filter and into the pump where it could damage the neoprene impeller. The discharge from the pump was returned to the flume behind the wave board so that the outflow would not affect the incident wave climate. Wave heights and profiles were recorded manually but much more frequently because of the smaller scale.

The bed material used for the beach pumping tests was a Fraser River Sand. The sieve analysis is shown in Figure 6.7. The beach was leveled to an initial profile and subjected to wave attack until equilibrium was attained and there was no observable change to the beach profile. At

this point the beach drain was activated and pumping initiated. The wave generator was run continuously throughout the test. Wave activity continued while the suction from the underdrain increased the infiltration capacity of the bed. When the beach had adjusted to a new steeper equilibrium, the underdrain was switched off and the final profile recorded.

In another experiment the process was cycled. Pumping induced onshore sediment transport on a stable, naturally draining beach. If pumping was stopped, the beach reverted to its original profile, and if restarted, assumed a steeper profile again.

The wave height used for these experiments was approximately 0.06 meters and the reflection coefficient was roughly 17 percent. The average measured discharge was 265 mL/s.

In another beach pumping experiment a bed made only of fine material was used to determine if both the fine and coarse materials experienced increased mobility from the infiltration-induced onshore shear stress. The bed material was again the Fraser River Sand, but the coarse fraction was sieved out. Sediment smaller than 0.3 millimeters was also discarded. A uniform, fine sand consisting only the material retained between the 0.3 and 0.6 millimeter sieves was retained for use and construction of the laboratory beach. The wave climate for this test was an incident wave height of 0.075 meters, a reflection coefficient of approximately 15 percent and a wave period of 2.2 seconds. The pump discharge was measured to be 360 mL/s.

The bed was leveled to the initial profile and waves attacked the beach until the profile reached an equilibrium. With the same wave attack, the pump was then turned on until the beach adjusted to a new equilibrium under these different infiltration conditions. When the pump was turned off, the beach reverted back to the original equilibrium profile for naturally draining conditions.

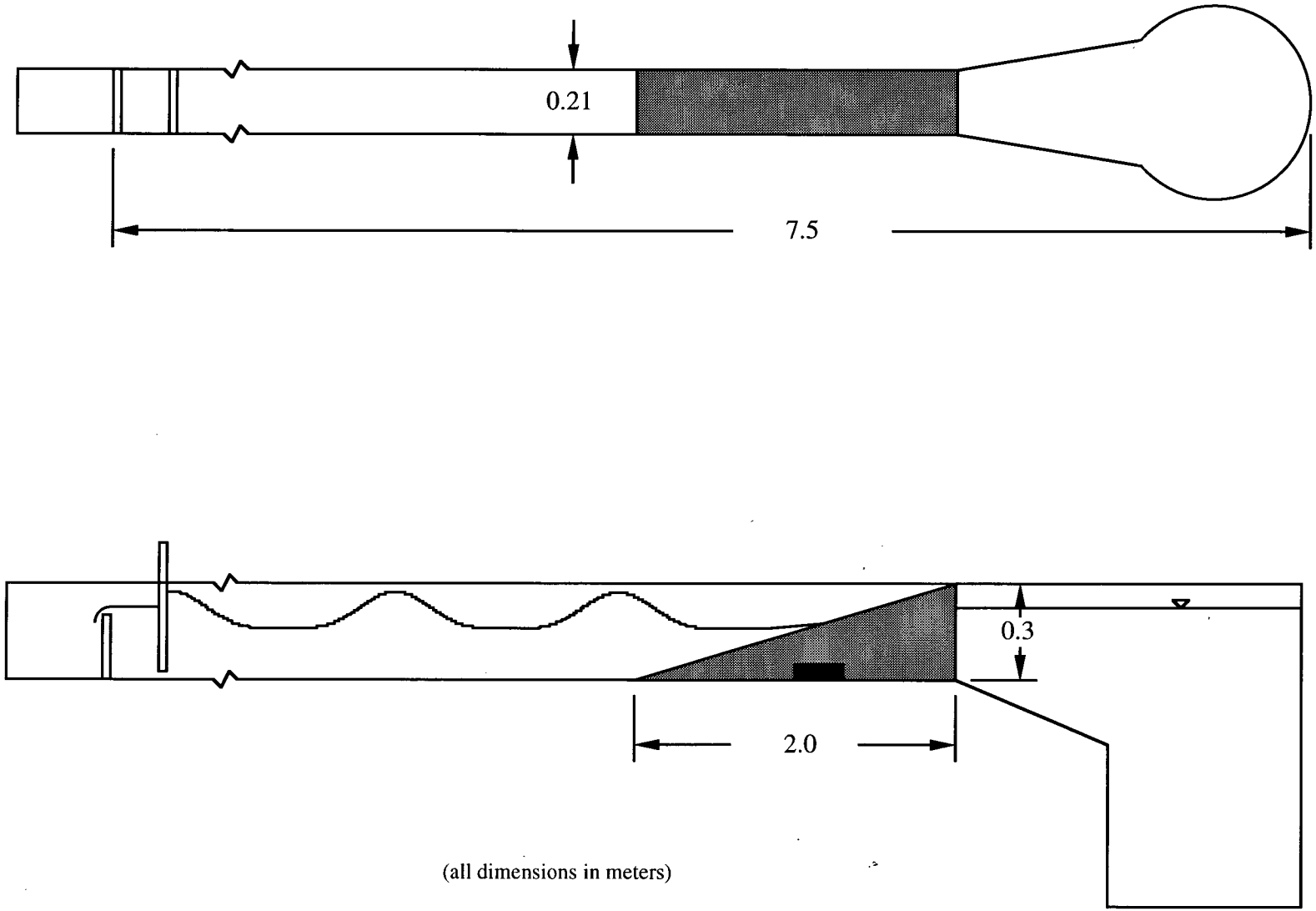

(all dimensions in meters)

Figure 6.6 Small Wave Flume

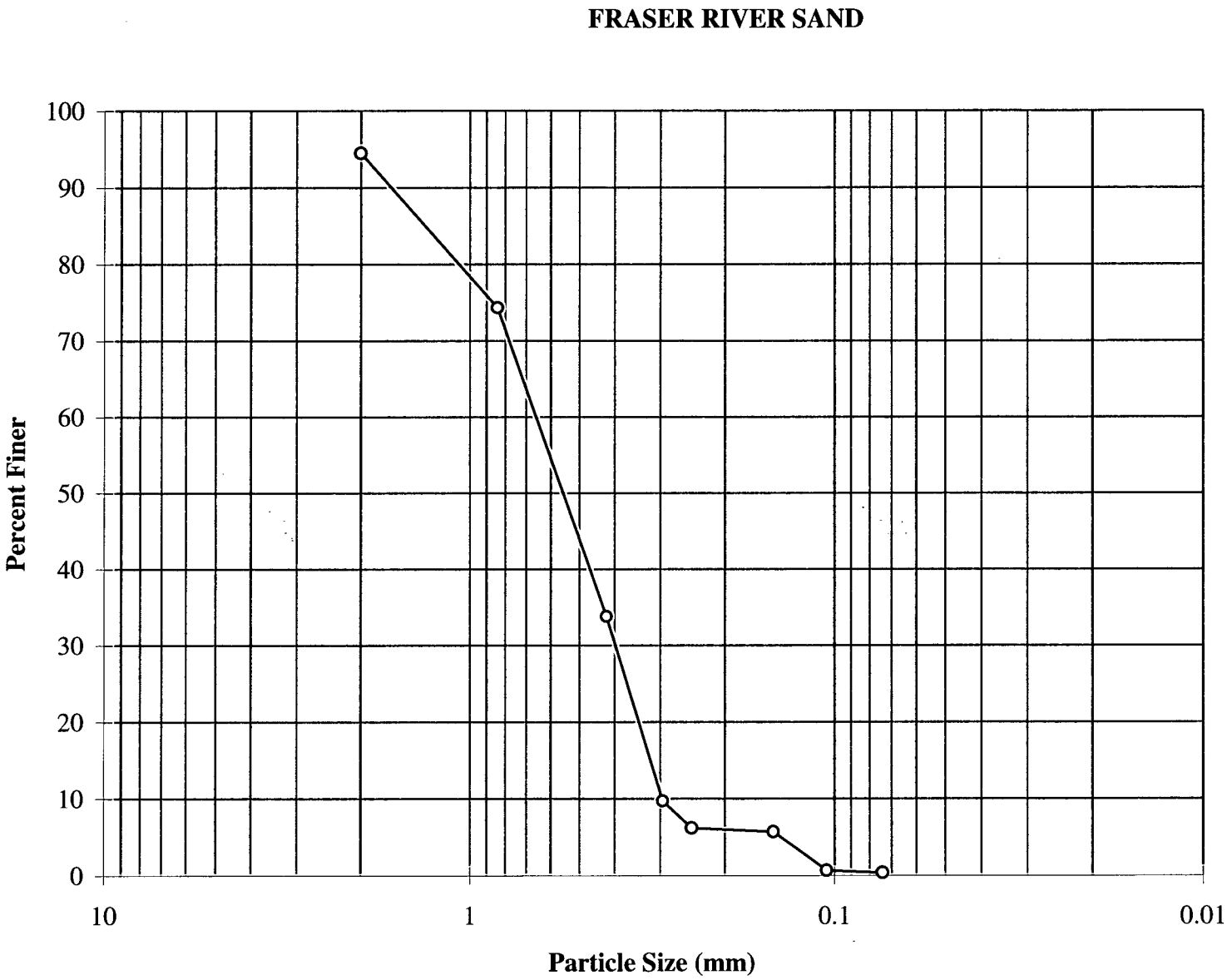

Figure 6.7 Particle Size Distribution of Sand Used in Pumping Tests

Chapter 7

Results and Discussion

7.1 Large Scale Tests: Sand and Gravel Mixtures

7.1.1 Effect of Initial Slope on the Equilibrium Profile

Figure 7.1 shows the results from two separate tests investigating the effect of the initial slope on the equilibrium profile of a beach made up of very fine gravel that did not contain any fine material. One test started with an initial profile that was flat and horizontal over a 2 meter section of the beach. The profile reached equilibrium after eight hours of wave attack. The equilibrium profile is shown in Figure 7.1. A large volume of material that was initially offshore was moved onshore to form a large protective berm and caused considerable steepening of the profile. The equilibrium profile was planar over most of the swash zone and was inclined at an angle of approximately 8.5 degrees. The slope of the offshore face of the breaker bar was roughly 33 degrees which is approximately equal to the angle of repose for this material.

In a second test, the initial slope was set at a value slightly less than the equilibrium slope reported in the above test. After only three hours of wave attack, the profile reached equilibrium. The final profile was nearly coincident with the equilibrium profile recorded previously for a horizontal initial slope. The positions of the berm and breaker bar were identical to the previous test and the stable slope angle was again 8.5 degrees. The similar profiles indicate that wave breaking at equilibrium was initiated at a particular location and in a particular depth of water for

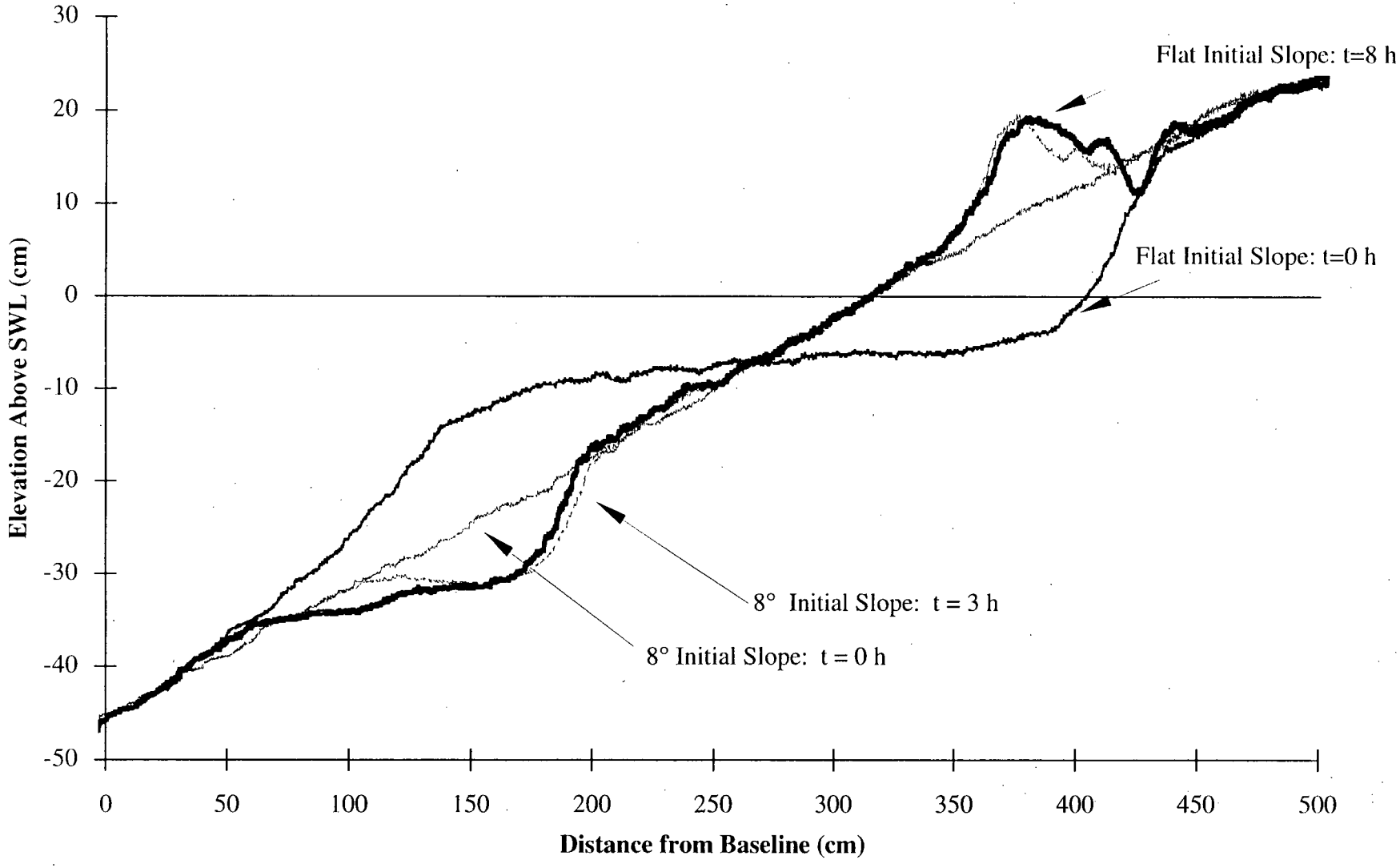

Figure 7.1 The Effect of Initial Slope on the Equilibrium Profile

both tests. Surf zone dynamics and shore processes were likely also similar because of the similarity between profiles. The results of these tests indicate that the initial slope has little influence on the final equilibrium profile.

7.1.2 Repeatability Between Tests

Tests were repeated under identical conditions to establish the level of reproducibility between tests and to determine the reliability of the testing procedure. Figure 7.2 shows the results of three separate tests conducted on a beach composed of only the coarse material. The wave height in all three cases was 0.2 meters. Superimposed records from three successive tests show the equilibrium profiles to be very similar. The equilibrium slope in the surf zone; the position and size of the berm and breaker bar; and the intersection of the still water line with the beach profile were all very similar. Figure 7.3 shows results from two successive tests repeated on a beach containing 25 percent fine material under identical conditions. The profiles are nearly coincident and show better repeatability than was attained for successive tests on the permeable beach. In general, successive tests repeated on the same bed material showed excellent reproducibility and equilibrium profiles that were almost identical. These results indicate that the careful testing procedure was very repeatable and that comparisons between tests were justified and reliable.

7.1.3 The Effect of a Larger Wave Height

Figure 7.4 shows the results from tests performed on a beach made up only of the coarse material. The initial slope in both tests was 8 degrees, but two different wave heights were used. One test used a 0.2 meter wave, while the other used a 0.25 meter wave to investigate the effect

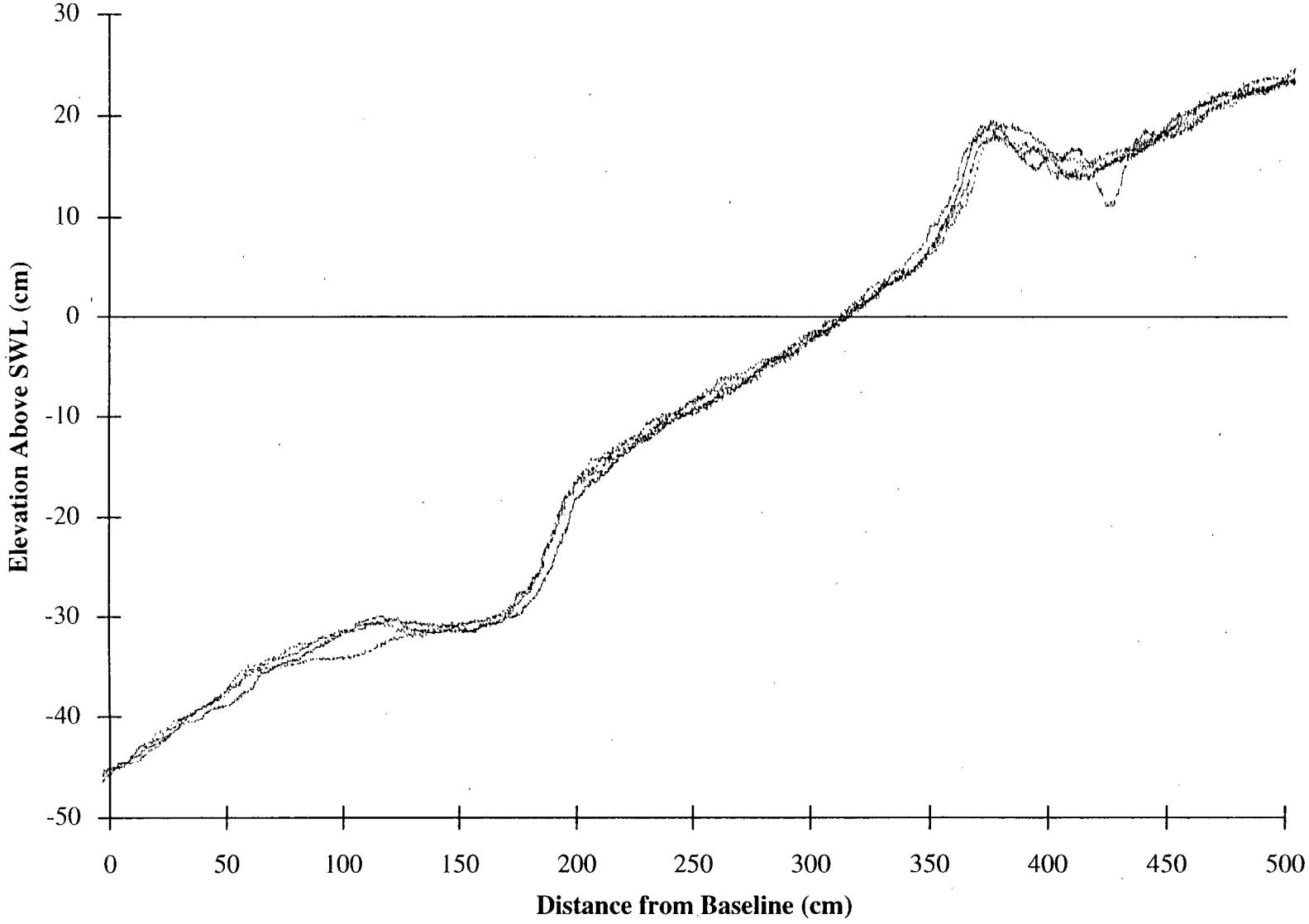

Figure 7.2 Superimposed Equlibrium Profiles: 0% Fines

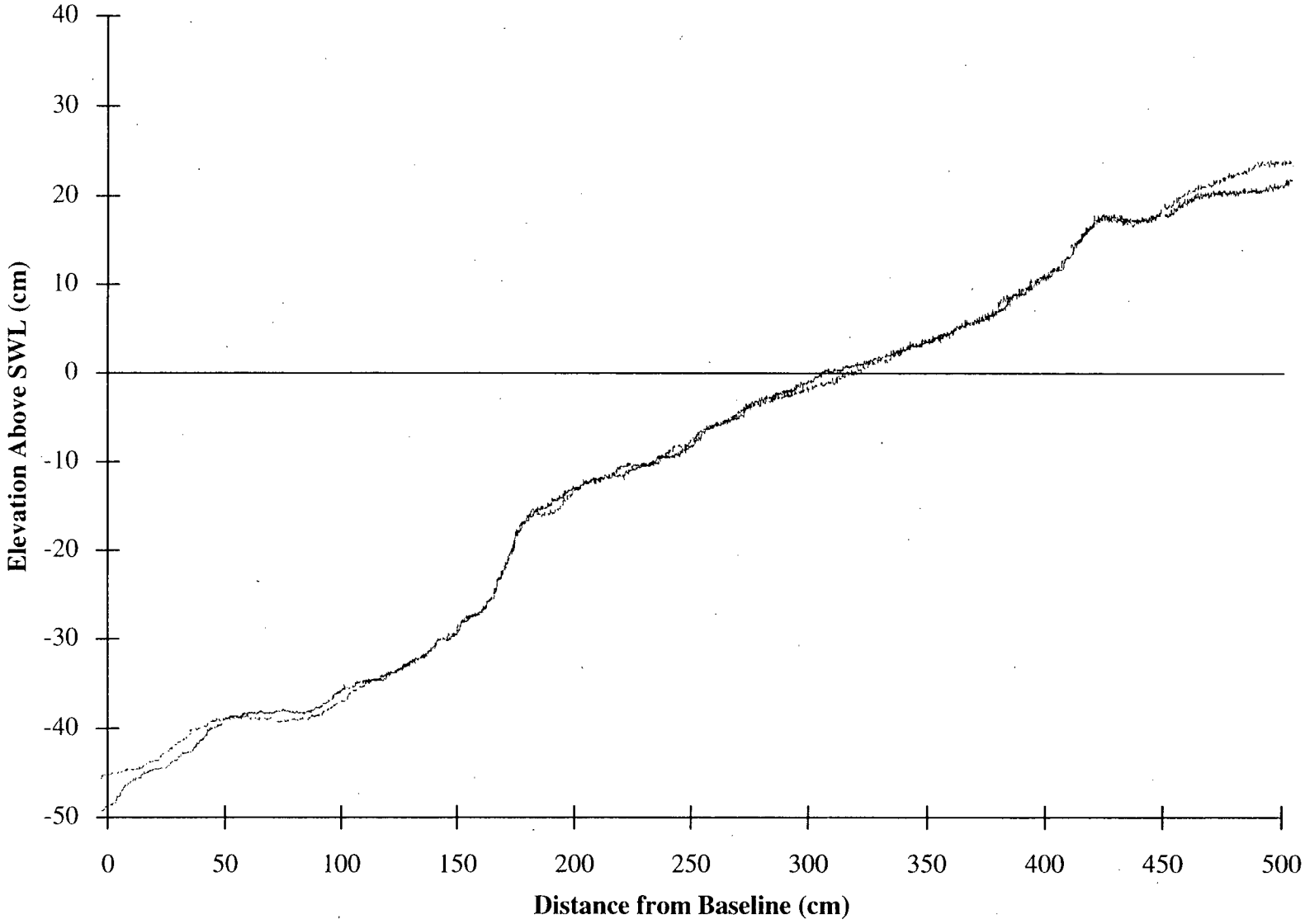

Figure 7.3 Superimposed Equilibrium Profiles: 25% Fines

of increasing the wave height on the equilibrium profile. The wave period was 2 seconds in both tests. The time required to reach an equilibrium condition was roughly the same. In both cases the profile stabilized between the second and third hour of wave attack. Equilibrium profiles for the two wave conditions showed some similarities, but as Figure 7.4 indicates, there were significant differences.

Comparing overlaid profiles shows that larger waves cause offshore movement and flattening of the beach profile. The onshore berm, although taller and pushed farther onshore from larger runup and stronger uprush, was eroded. The breaker bar was farther offshore and enlarged - probably with material from the eroded berm. Wave breaking was initiated farther offshore and in deeper water for the larger wave. Offshore of the breaker bar, the larger wave dislodged material to a proportionately greater depth than did the smaller wave. The two previous observations can most likely be explained with by an argument incorporating the concept of the breaker index. Secondary wave breaking scoured a portion in the mid-profile. This effect is not likely to exist for random wave that would smooth out such an irregularity.

7.1.4 The Effect of Changing Bed Permeability and Gradation

The equilibrium profiles for beaches with different sediment gradations made of very fine gravel combined with 0, 5, 15 and 25 % fine sand subjected to the same wave attack are shown in Figure 7.5. The initial profile for every test was 8 degrees, and the wave height used in each case was 0.2 meters. Because the initial slope was close to the final equilibrium profile, these tests reached equilibrium after less than 3 hours of continuous wave attack.

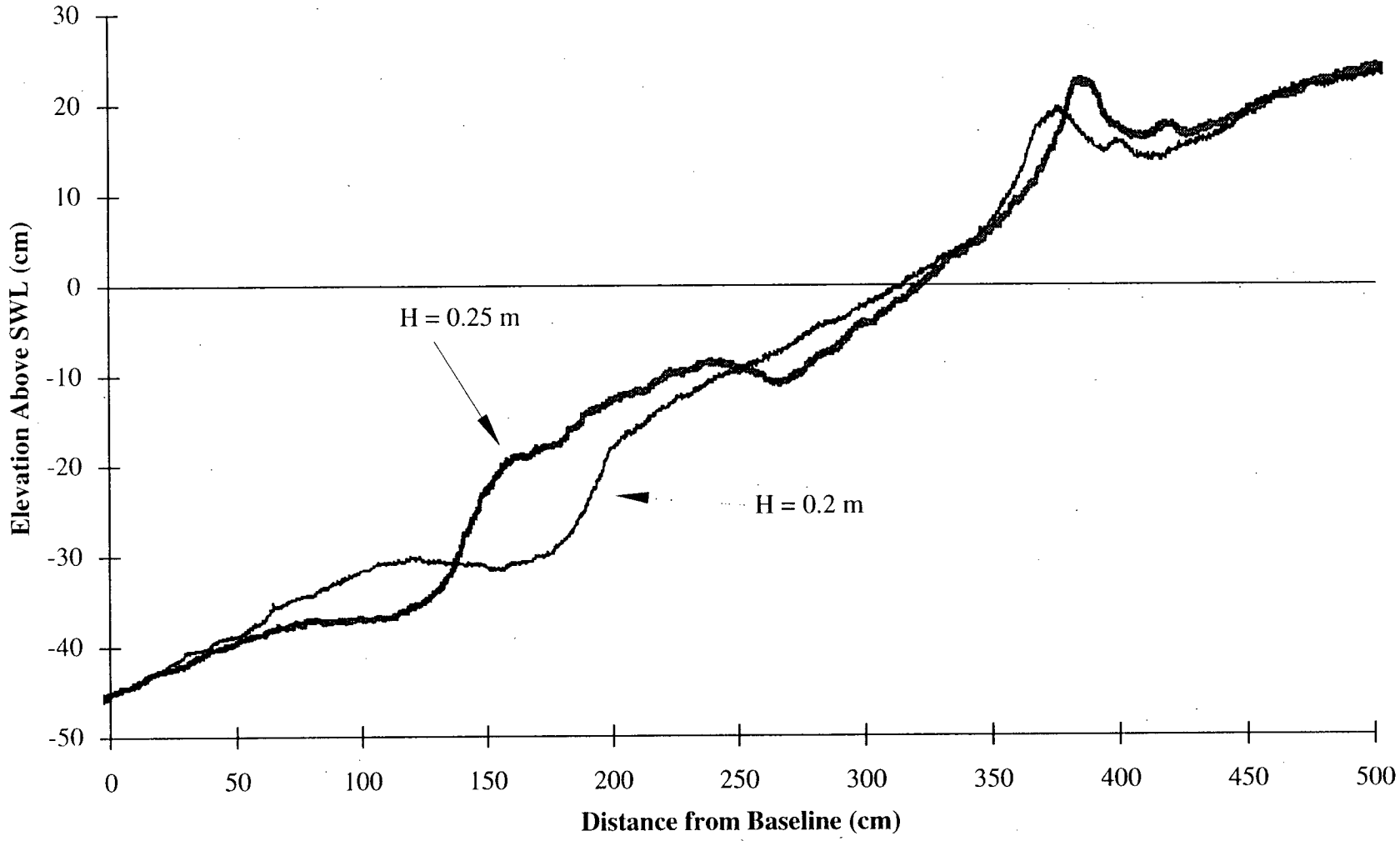

Figure 7.4 The Effect of a Larger Wave Height

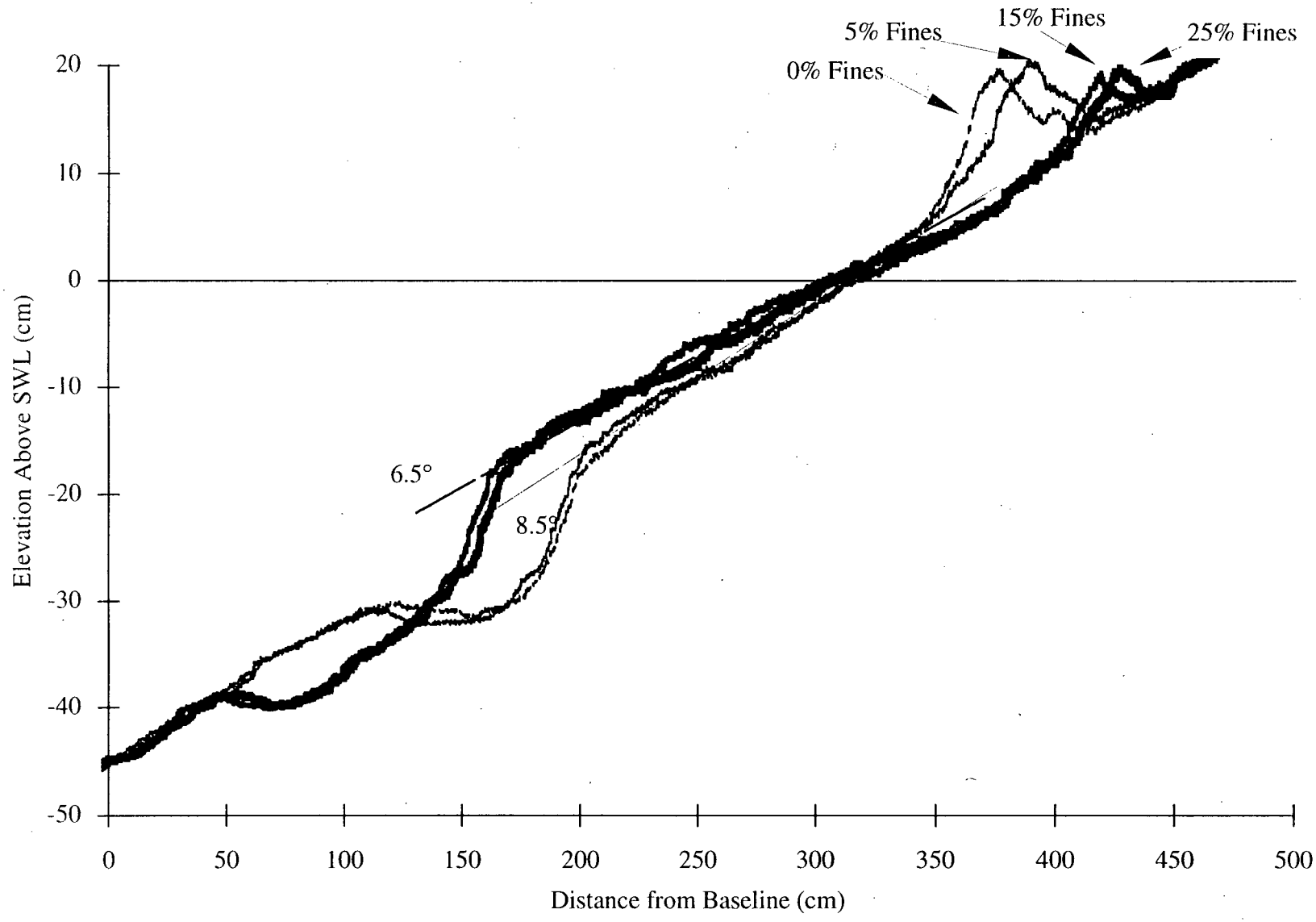

Figure 7.5 Equilibrium Profiles

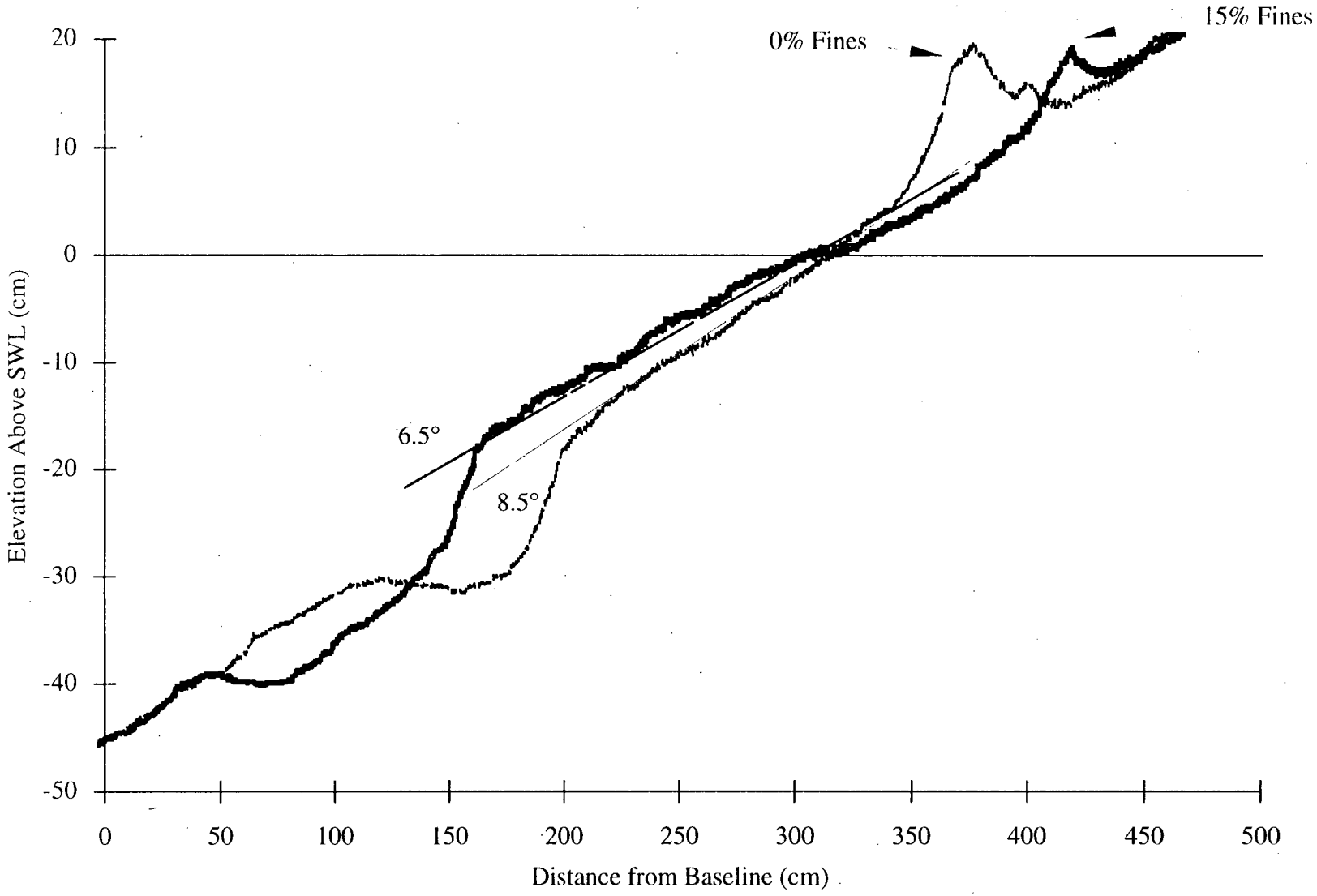

Figure 7.6 Equilibrium Profiles for Permeable and Impermeable Beaches

7.1.4.1 Highly Permeable Beaches

The equilibrium profile for a bed made entirely of very fine gravel and a bed containing just 5 % fine sand are quite similar. The slope is relatively steep and is approximately constant at 8.5 degrees (1:7) for most of the surf zone. The position and size of both the berm and breaker bar were nearly identical for these two tests. The hydraulic conductivity of these two materials is quite similar and 5 % of fines does not change the permeability significantly. Wave action on and in these two beaches would be very similar; and more importantly, the backrush would be of equal intensity. For both 0 % and 5 % fines, infiltration helps to steepen the equilibrium profile and constructive wave action moves material from the breaker bar onshore to build a large berm.

The injection of dye into the porous beach revealed that the velocity vectors were predominantly parallel to the beach face for these relatively permeable materials and that the flow field was contained within the upper layers and did not penetrate very deep into the beach. Approximate values of the seepage velocity were estimated from streamlines that revealed the flow paths. An average value of approximately 1 cm/s was representative.

Water surface elevation records did not indicate that wave reflection was significant on these permeable beaches.

7.1.4.2 Reduced Permeability Beaches

The equilibrium profiles from tests that increased the proportion of fines in the bed material are also presented in Figure 7.5. The results from tests that used 15 and 25 % fines also show considerable similarity to one another. The equilibrium profiles are nearly identical. Insufficient infiltration contributes to a net offshore stress that carries material seaward. The

erosion of the berm and offshore extension of the breaker bar lengthens the surf zone and flattens the equilibrium profile. The slope angle was reduced to 6.5 degrees (1:9). Stronger uprush penetrated farther into the foreshore region and eroded the beach berm. Run-up levels were relatively unchanged from values observed for tests on more permeable beaches.

Figures 7.5 and 7.6 indicate that there is a critical percentage of fines which is sufficient to change the permeability so that further addition causes no further effect. From these experiments, it seems that the threshold is approximately 15 percent. Adding fines did not cause significant shoreline retreat, although a considerable volume of material was transported across the surf zone as the beach profile appeared to pivot about a point near the shoreline.

Dye injection against the flume wall indicated that the flow field penetrated deeper into the bed before emerging near the break point. Dispersion appeared to be almost as effective advection for transport of the tracer. Streamlines indicated that the mean velocity was not parallel to the beach face but revealed a vertical tendency. The seepage velocities were considerably reduced based on estimates of 0.2 to 0.3 cm/s.

Water surface elevation records indicated increased wave reflection from impermeable slopes which dissipate much less energy through wave damping and percolation losses than do permeable beaches. The wave records are presented and discussed later in this chapter.

Some material segregation at the interface was observed. A thin layer on the surface of the bed was cleaned of fine material originally present in the mixture. It is uncertain whether the fines were forced deeper into the bed or if the sediment was entrained into the surface flow and carried away. The migration of fines into the bed could have been forced by wave slamming on the beach in a way similar to piping. Entrainment would have most likely been due to the higher levels of turbulence due to wave breaking which increases sediment suspension.

7.1.4.3 Wave Reflection and Long Wave Generation

Visual observations and probe records indicated that the wave climate became increasingly confused and less monochromatic as the permeability of the bed decreased and the beach slope flattened. The water surface elevation showed consecutive large and small waves that, upon breaking were manifested as alternating "high" and "low" run-up levels. A time-series spectral analysis showed a significant amount of energy at a frequency of half the incident wave period that was not present for permeable beaches. This indicated that reflection was increasing and suggested either long-wave generation through swash interactions or resonance between the beach and wave board. Whatever the mechanism, the "dichromatic" wave traces and beats that accompanied the reduction of bed permeability were characteristic of increased reflection. The frequency downshift was not observed for permeable beaches which indicates that the magnitude of the reflected wave depends on the characteristics at the partially reflective boundary such as the slope, length and permeability of the beach.

The interaction of the swash oscillations with the incoming breaker affects the timing and position of wave-breaking. Swash interactions can also generate long waves that, when superimposed on the incident wave field, produces the observed water surface through partial

constructive and destructive interference. Diminished backwash provides less resistance to the surging breaker and facilitates higher run-up; while powerful backrush impinging on the incoming breaker makes it plunge earlier and in deeper water which affects the position of the breaker bar. The frequency downshift of swash oscillations has been studied by Mase (1994). Whether it is uprush-backwash interactions or standing long waves that dominate swash oscillations depends on the power of the incoming waves. Low frequency uprush-backrush dominate swash oscillations when the incoming wave power is large. Perhaps the energy lost to percolation is enough to reduce the incoming wave power so that swash oscillations were long wave dominated and less severe.

A reflection coefficient of 18-20 percent confirms that less permeable beaches are more reflective. The water surface records and spectral density analysis for a permeable and an impermeable beach are presented in the figures that follow. Figure 7.11 is a wave recorded that wave generated by superimposing an incident wave (H = 0.2 meters) with an out of phase reflected long wave ($L_i/L_r = 0.5$, $K_r = 0.2$, $\varepsilon_r = \pi/4$). This simulated wave trace is similar to the time series records.

7.2 Small Scale Tests: Beach-face Pumping and Underdrains

7.2.1 Infiltration Induced Accretion and Profile Steepening

The results from Pumping Test A are presented in Figure 7.12. The plot shows equilibrium profiles for pumped and unpumped conditions. Figure 7.12 indicates that infiltration had a major control on the equilibrium profile. The equilibrium profile formed under increased

infiltration conditions was considerably steeper than the beach profile that was formed under natural drainage conditions. The pumped equilibrium profile was inclined at 15 degrees; while under natural drainage conditions the stable beach slope was only 10 degrees. Presumably, increased infiltration is responsible for the slope increment.

A large amount of material from the breaker bar was carried onshore by wave action and deposited in the foreshore. The stable position of the breaker bar was considerably closer to shore, even though the shape and slope of the breaker bar were unchanged. Neither shoreline advance nor shoreline retreat was observed to any large degree. The pumped equilibrium profile seemed to pivot about a point close to the intersection of the still water line and the beach.

Outside the break point, the pumped and unpumped profiles were similar. Sediment transport activity was low and was apparently unaffected by changes to infiltration conditions in the surf zone. Breaking waves did penetrate slightly further inshore because of the erosion and onshore movement of the breaker bar.

Video records shows that onshore sediment movement was erratic and occurred in pulses. Slugs of material migrated up the beach from the breaker bar to the foreshore region. The surges of sand occurred as discrete events.

Calculations indicate that the volume of sand contained within the test section was the same for both infiltration conditions which confirms conservation of sand mass.

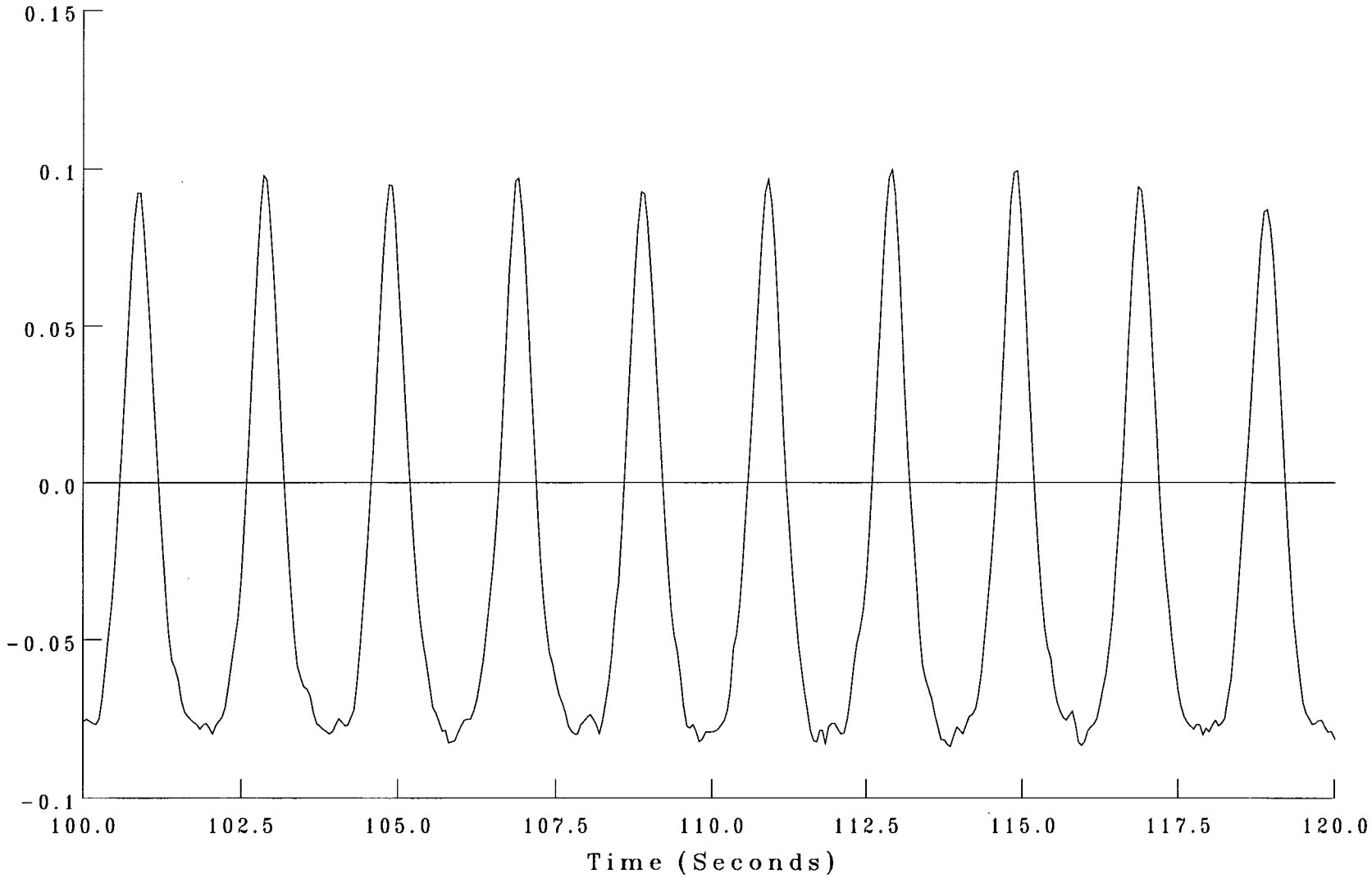

Figure 7.7 Deep Water Wave Record for a Permeable Beach (0% Fines), t=45 min

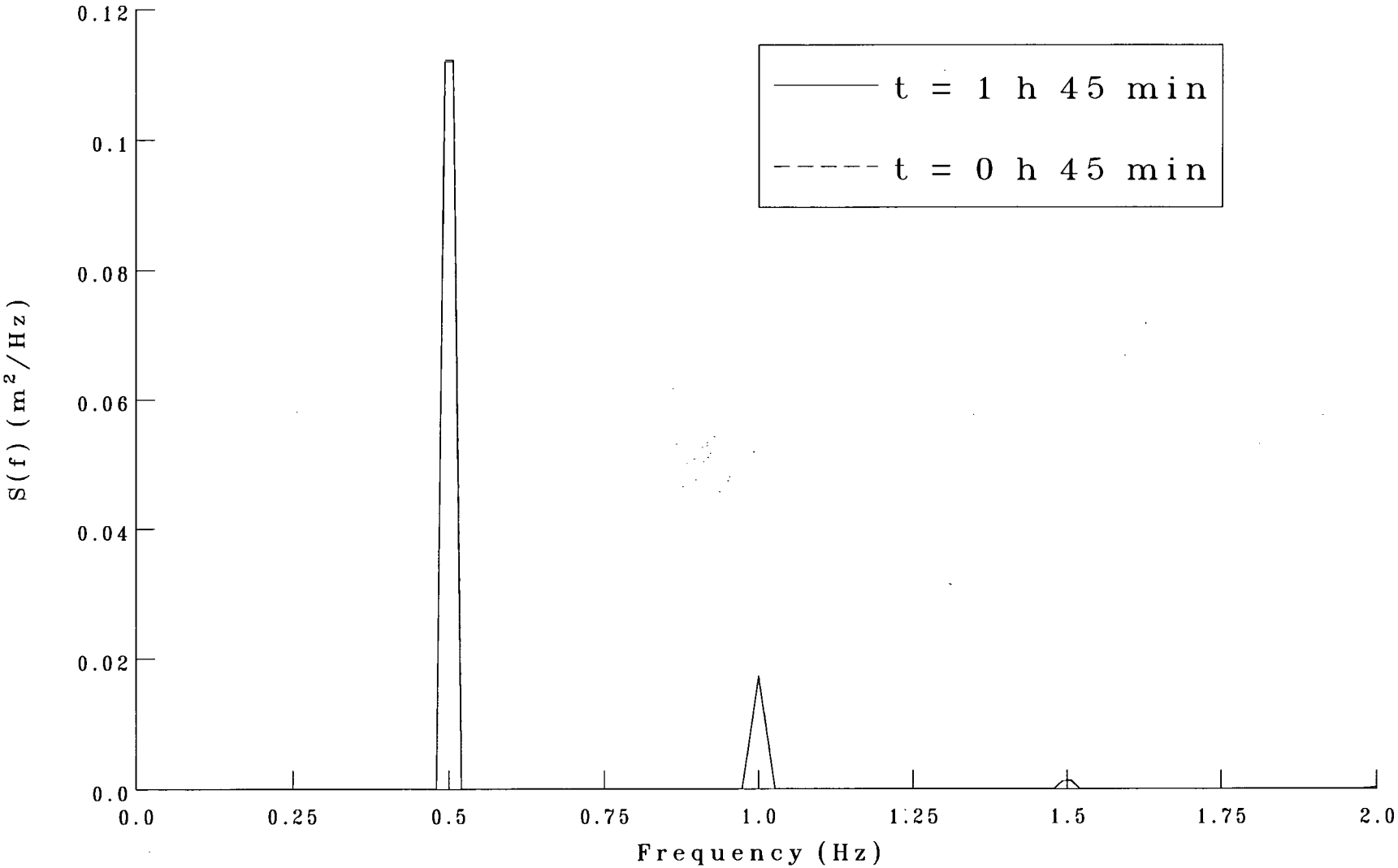

Figure 7.8 Spectral Density from the Deep Water Wave Record for a Permeable Beach (0% Fines)

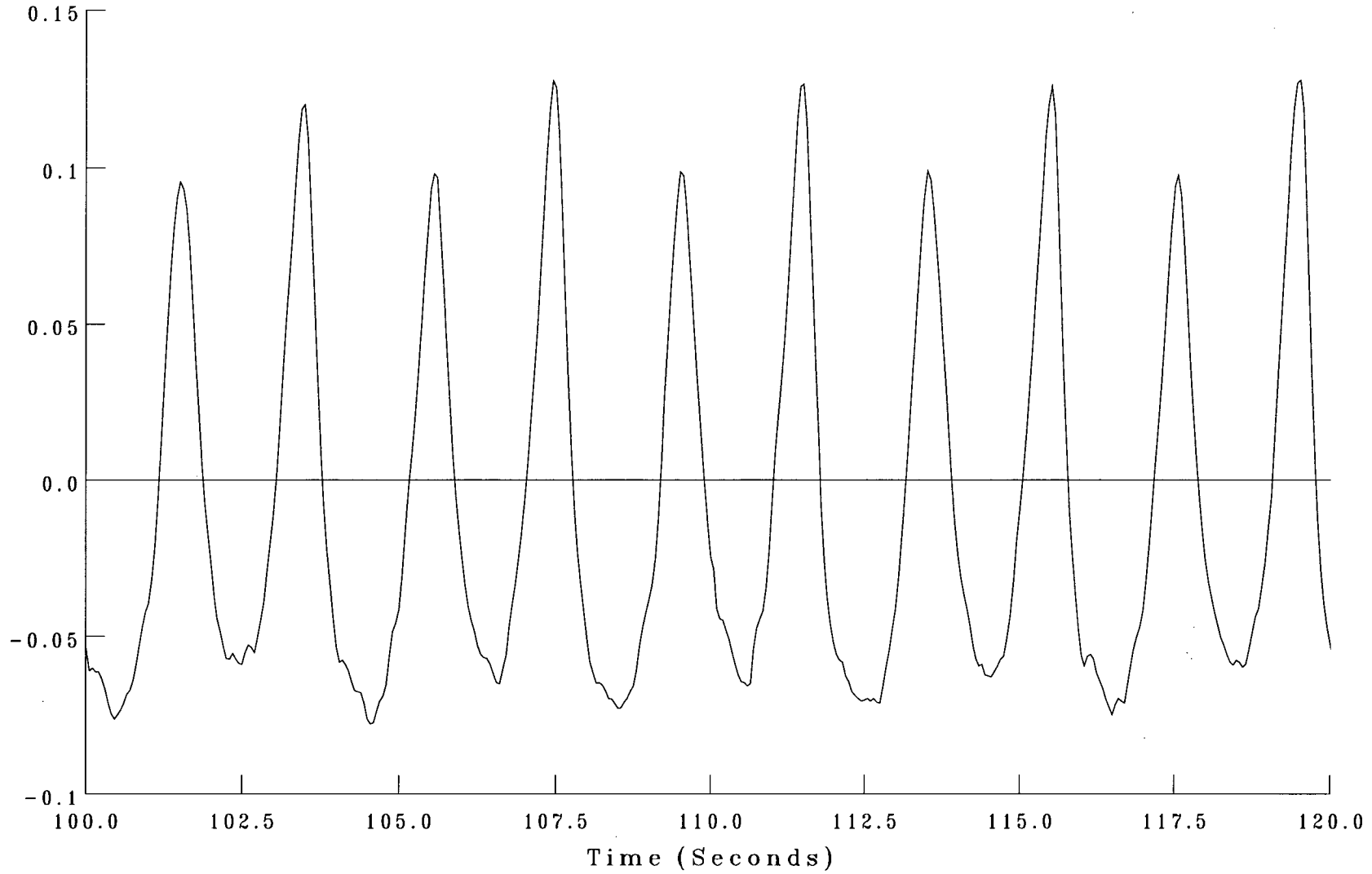

Figure 7.9 Deepwater Wave Record for an Impermeable Beach (25% Fines), t=45 min

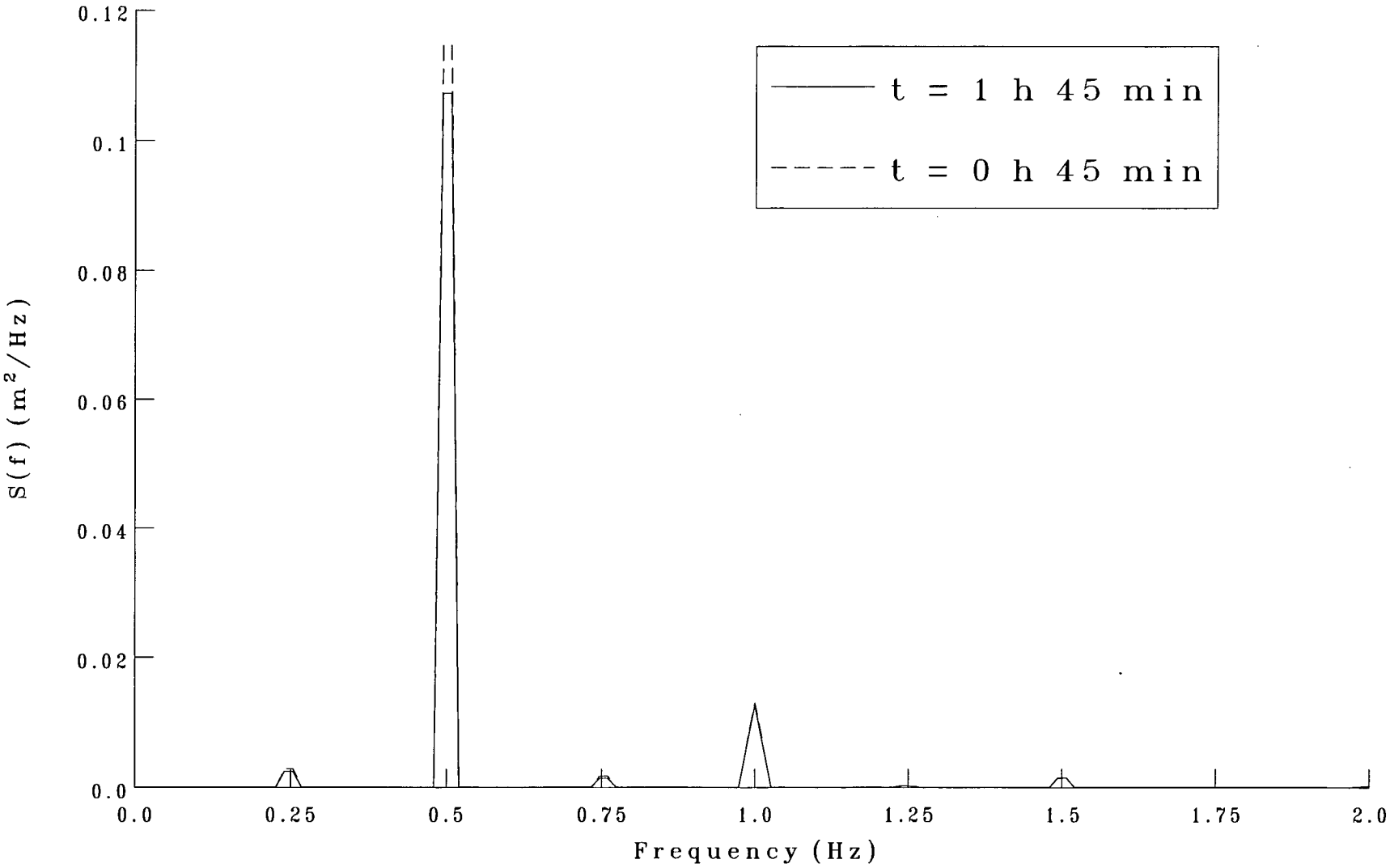

Figure 7.10 Spectral Density from the Deep Water Wave Record for an Impermeable Beach (25% Fines)

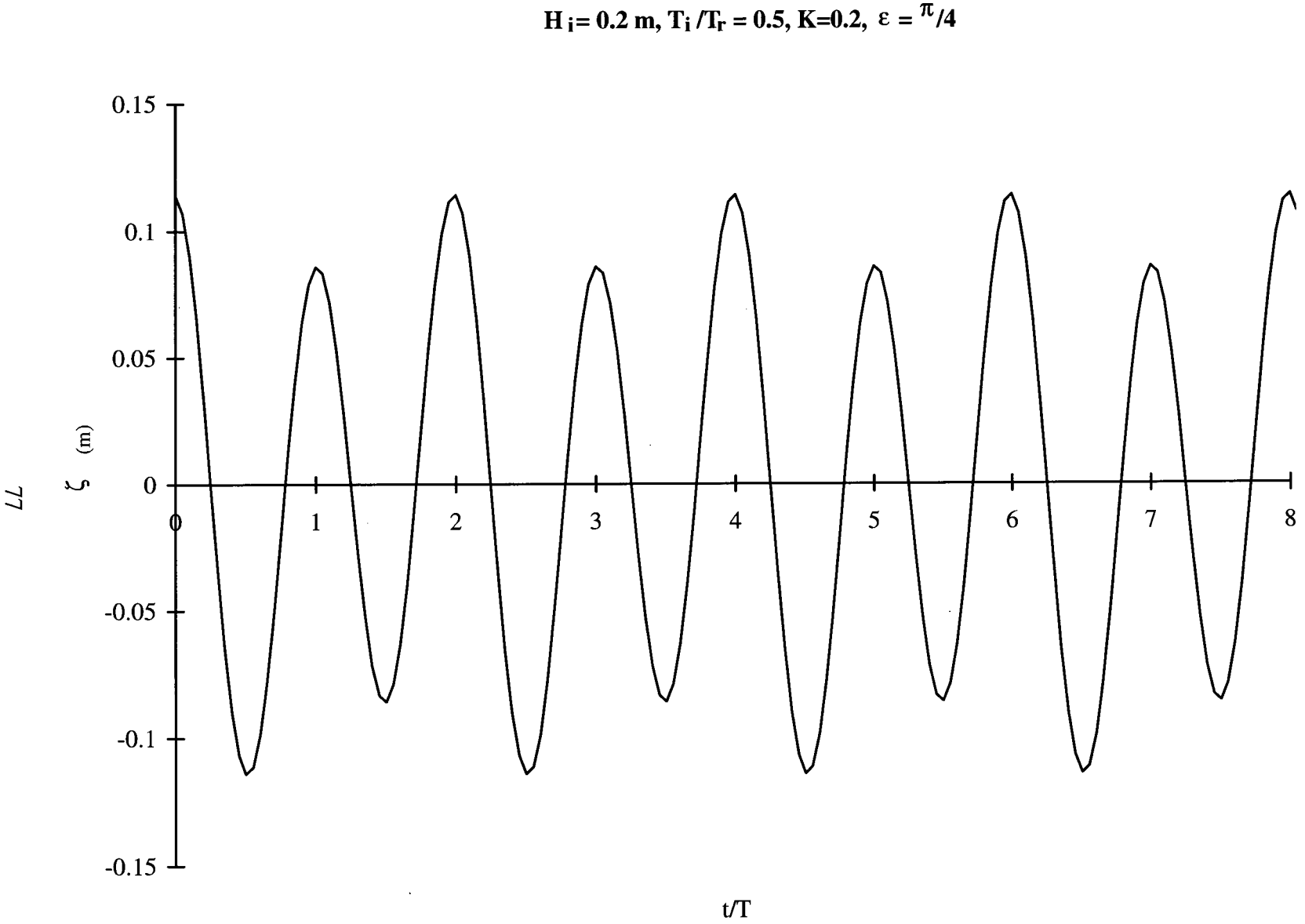

Figure 7.11Simulated Wave Record

7.2.2 Cyclic Pumping and Reversibility

Pumping Test B investigated the reversibility and reproducibility of the onshore sediment transport induced from increased infiltration. The results are shown in Figure 7.13. The experiment indicates the steepening to be reversible and repeatable when the beach was subjected to cycles of pumping followed by natural drainage. Subsequent pumped profiles were nearly coincident, and unpumped profiles appear to be identical. The adjustment process was fairly rapid and was for the most part complete within thirty minutes of wave action.
The tests suggest that there exists a stable beach profile that is unique for a certain amount of infiltration. The uprush induced onshore sediment transport is balanced exactly by an equivalent amount of offshore material movement from the backrush cycle to yield no net transport.

Longshore variation in the amount of pumping induced accretion was observed and is shown in Figure 7.14. The effect was most pronounced in the foreshore section. Some variability is natural and can be attributed to inadequacies of the experiment. The steepest slope angles over the entire beach were much greater than the average values reported in the previous figures that were supposed to be representative of the whole beach. Some slope angles in the foreshore reached as much as 20 degrees (1:3). This means that the accretion is much more pronounced for some sections of the beach and the effect of beach pumping is much more significant than at other sections.

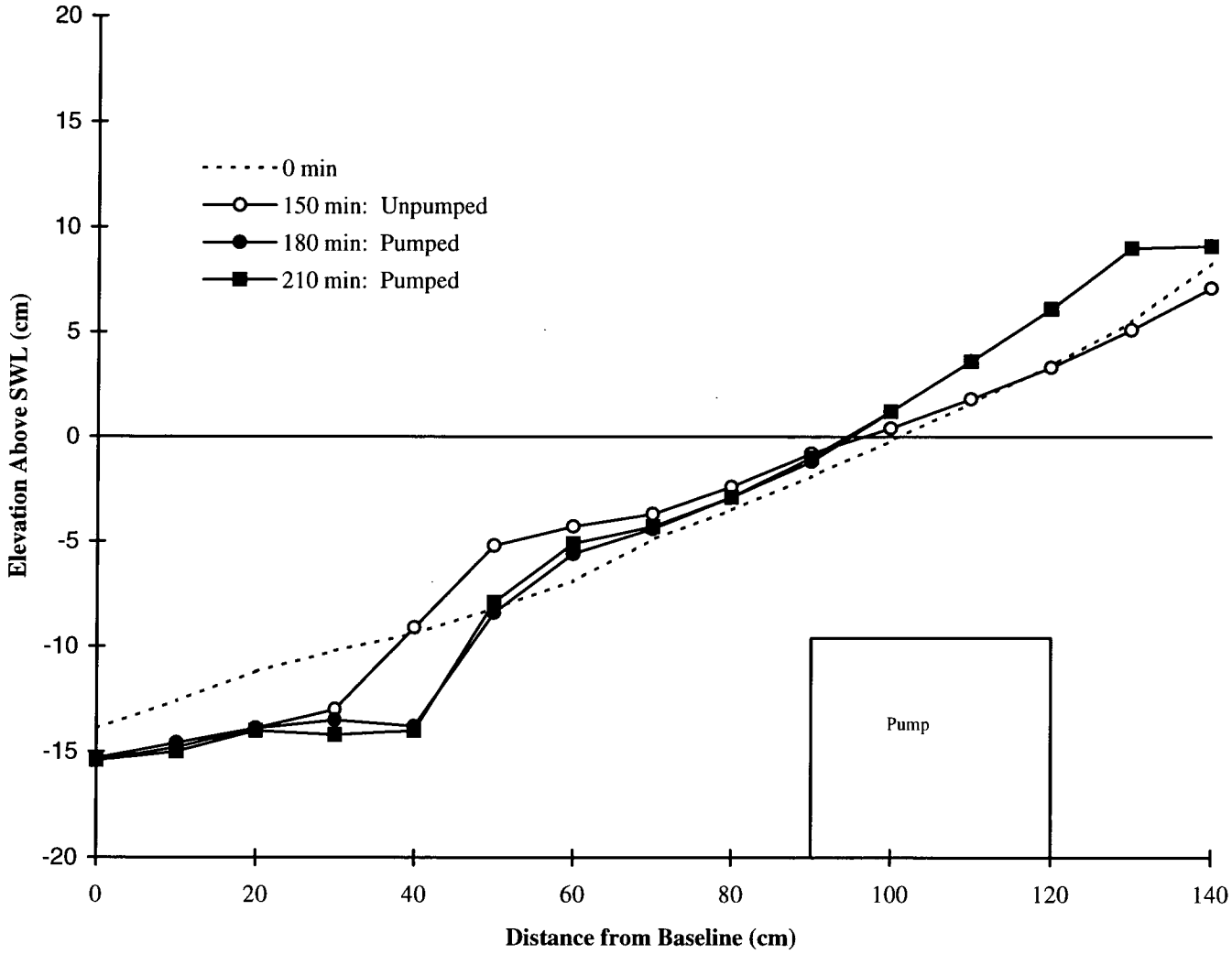

Figure 7.12 Pumped and Unpumped Equilibrium Profiles (Test A)

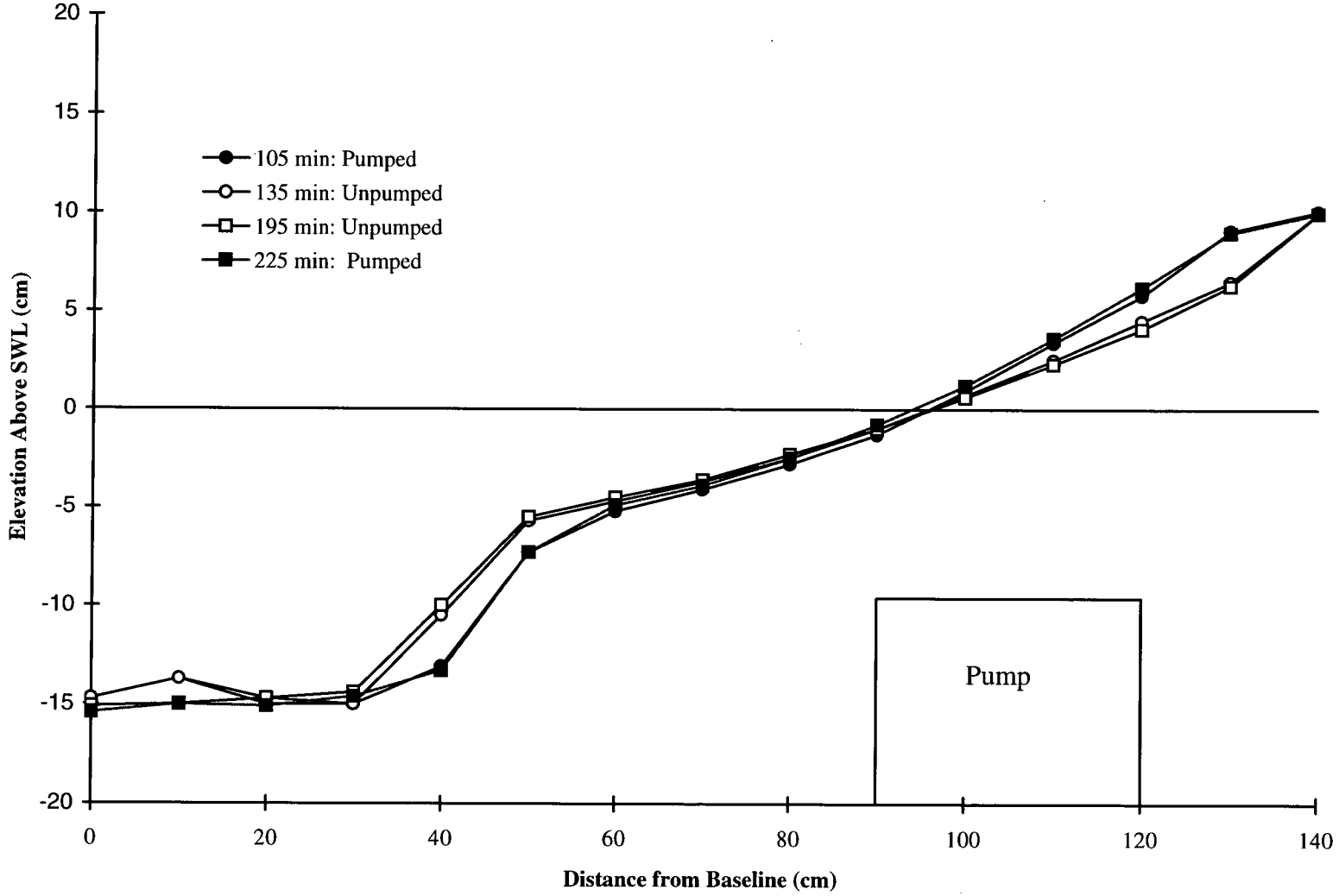

Figure 7.13 Pumping Cycles: Equilibrium Profiles (Test B)

7.2.3 Fine Bed Material

The results from Test C studying the effect of increased infiltration by pumping on a beach made of a uniform fine sand are shown in Figure 7.15. The pumped profile was steeper than the equilibrium profile which occurred under natural drainage conditions. Onshore movement of material from the breaker bar to the berm and foreshore accretion was consistent with Tests A and B which used the entire gradation of Fraser River Sand. The slope angle over most of the surf zone is 14 degrees (1:4). This value does not change significantly with increased infiltration. The pumped and unpumped slope angles are quite similar. Slope angles in the foreshore are significantly higher because of the formation of the protective berm and foreshore accretion. The slope angle was as much as 32 degrees (1:1.6) which was approximately the angle of repose for this material. Figure 7.15 shows some shoreline advance under increased infiltration during pumping, but it is small.

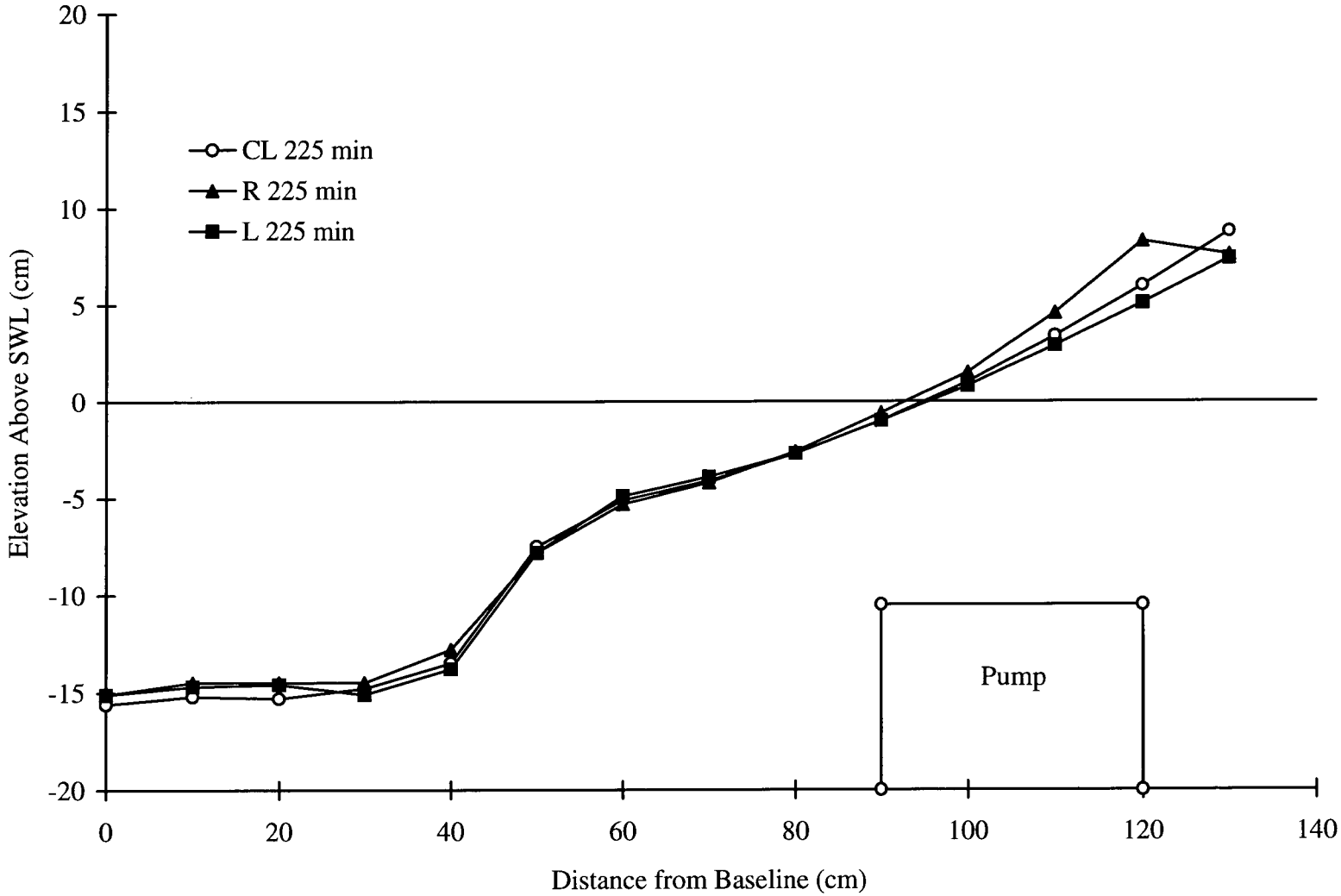

Figure 7.14 Longshore Variation in Pumped Equilibrium Profiles (t=225 minutes)

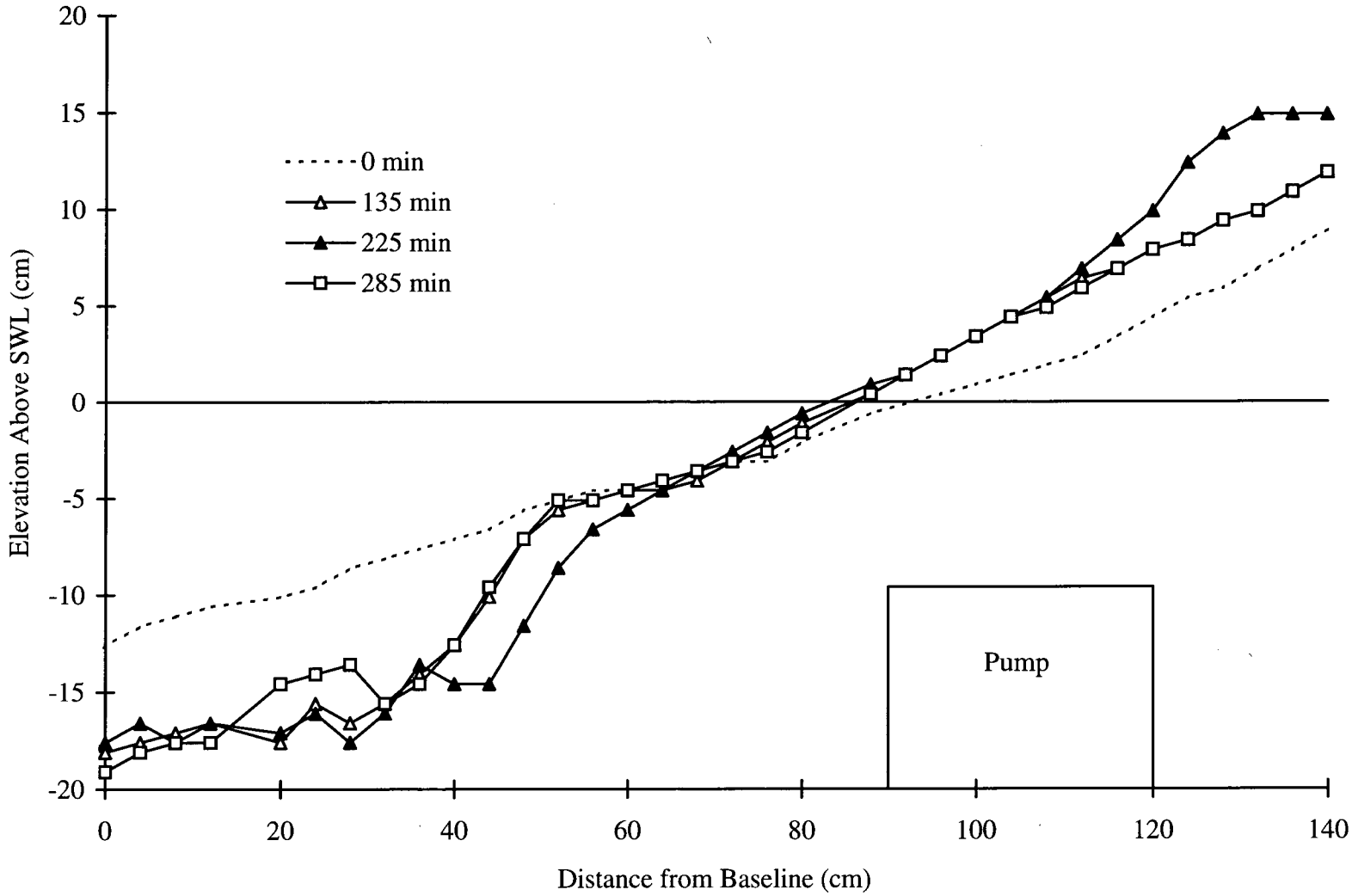

Figure 7.15 Pumped and Unpumped Equilibrium Profiles (Fine Material)

Chapter 8

Summary and Conclusions

The purpose of this study was to determine the effects of infiltration on cross-shore sediment movement and the equilibrium beach profile. The experiments demonstrate clearly that infiltration is a major control on the beach profile and equilibrium slope. These findings confirm theoretical predictions that infiltration promotes onshore sediment movement and increases the net onshore shear stress. Changes in beach permeability and drainage affect the stability and position of features such as the breaker bar and beach berm.

Hydraulic model tests show considerable differences between permeable and impermeable beaches. Experiments show that highly permeable beaches are steeper than beaches of reduced hydraulic conductivity. Changes to material permeability which results in reduced infiltration cause offshore sediment transport and reduce the equilibrium beach slope.

Beaches made of very fine gravel that are clean and uniform in composition are 30 % steeper than less permeable beaches that contain as little as 15 % fine material. There is a critical percentage of fines that changes the permeability of the bed which in turn affects the beach slope and equilibrium profile. Additional fine material causes no further effect. The experiments indicate that the critical value is approximately 15 percent fines. This is in approximate agreement with empirical equations which correlate permeability with grain size.

Artificially induced infiltration by beach face pumping is shown to contribute to improved stability and maintain material onshore to safeguard against foreshore erosion.

Increased infiltration by pumping contributes to an onshore shear stress which initiates immediate onshore sediment movement and steepens the equilibrium profile which promotes foreshore accretion.

Measurements show that infiltration conditions affect wave reflection and the flow field within the porous beach.

Analysis of water surface records indicates that impermeable beaches are more reflective than permeable slopes. Presumably, permeable beaches dissipate more incoming wave energy through percolation than do impermeable beaches.

Dye injection indicates that seepage velocities within permeable beaches are larger than velocities within impermeable beaches. Tracers penetrate deeper into a permeable beach before emerging near the break point. The flow field in a permeable structure is largely confined to the surface of the bed.

Chapter 9

Recommendations for Further Study

More work should be done to determine the validity of these findings for a wider range of wave heights and periods. Experiments could be conducted in a flume with active wave absorption to reduce the effects of wave reflection and resonance.

Future investigations should include measurements of the friction angle of the sand mixtures to determine to what extent the addition of fine material is affecting the angle of repose and shear strength of the beach material.

The small scale beach pumping tests need to be carried out at a larger scale where the proper facilities exist to determine the optimum pumping characteristics such as flow rate, and suction head. Varying the elevation and cross-shore position of the intake would also lead to improved designs of beach management systems.

Large physical model tests should be performed with more reliable pressure measurements complemented with velocity records and water surface elevations to produce a comprehensive data set for calibration of a numerical model.

A numerical model should be developed which couples the surface and internal flow regions, perhaps using some of the theory from the earlier sections of this dissertation. This model could be used to predict the observed phenomena and the effect of varying wave conditions, beach material, drainage, and beach slope. Practicing engineers would also benefit from the improved understanding of infiltration effects on profile stability and prediction.

Bibliography

Adams, J.W., 1989. The Fourth Alternative -- Beach Stabilization By Beachface Dewatering. Coastal Zone '89, Proc. of the 6th Symposium on Coastal and Ocean Management, Charelston, South Carolina, vol. 4: 3958-3974.

Ametepe, J.K., 1991. A Model of Longshore Transport Rate. Master of Applied Science Thesis, The University of British Columbia.

Bagnold, R.A., 1963. Beach and Nearshore Processes. In: M.N. Hill (Editor), The Sea, Interscience, New York, vol. 3: 507-528.

Bagnold, R.A., 1941. Beach formation by Waves; Some Model-Experiments in a Wave Tank. Journal Institution of Civil Engineers: 27-52.

Bowen, A.J., Inman, D.L. and Simmons, V.P., 1968. Wave 'Set-Down' and Set-Up. Journal of Geophysical Research, vol. 73, No. 8: 2569-2577.

Chappell, J., Eliot, I.G., Bradshaw, M.P. and Lonsdale, E., 1979. Experimental Control of Beach Face Dynamics by Water-Table Pumping. Engineering Geology, vol. 14: 29-41.

Collins, J.I. and Chesnutt, C. B., 1975. Tests on the equilibrium profiles of model beaches and the effects of given shape and size distribution. ASCE, Proc. Symp. on Modelling Techniques, San Francisco, California: 907-926.

Davis, G., Hanslow, D., Hibbert, K. and Nielsen, P., 1992. Gravity Drainage: a New Method of beach Stabilization Through Drainage of the Watertable. Proc. 23rd International Conference on Coastal Engineering, Venice, Italy, Paper No. 100: 209-210.

Elliott, T.R. and Quick, M.C., 1995. The Influence of Infiltration on Cross-shore Sediment Transport. Proc. Canadian Coastal Conference, Dartmouth, Nova Scotia. In Press.

Finn, W. D., Siddharthan, R., and Martin, G. R., 1983. Response of Seafloor to Ocean Waves. Journal of Geotechnical Engineering, ASCE, vol. 109, No. 4: 556-572.

Gaythwaite, J.W., 1990. Design of Marine Facilities for the Berthing, Mooring and Repair of Vessels. Van Nostrand Reinhold, New York, New York.

Granthem, K.N., 1953. Wave Run-up on Sloping Structures. Trans. American Geophysical Union, vol. 34, No. 5: 720-724.

van Gent, M.R.A., 1994. The Modelling of Wave Action on and in Coastal Structures. Coastal Engineering, vol. 22: 311-339.

Gourlay, M.R., 1980. Beaches: Profiles, Processes and Percolation. Proc. 17th Coastal Engineering Conference, Sydney, Australia, vol. 2: 1320-1339.

Hall, K.R., 1990. Numerical Solutions to Wave Interaction with Rubblemound Breakwaters. Canadian Journal of Civil Engineering, vol. 17: 252-261.

Hannoura, A.A. and Barends, F.B., 1981. Non-darcy Flow; A State of the Art. Proc. Euromech 143, Delft: 37-51.

Hansen, H. K., 1986. Coastal Drain System: Full Scale Test at Thorsminditangen. Summary Report Number 170-83322, Danish Geotechnical Institute, Lyngby, Denmark.

Har, B.C., 1984. A Shoreline Prediction Model. Master of Applied Science Thesis, The University of British Columbia.

Hattori, A., Sakai, T. and Hatanaka, K., 1992. Wave-Induced Transient Pore-water Pressure and Seabed Instability in Surf Zone. Proc. 23rd International Conference on Coastal Engineering, Venice, Italy, Paper No. 196: 405-406.

Hazen, A., 1911. Discussion of: Dams in Sand foundations, by A.C. Loenig, Trans. ASCE, vol. 73: 177-199.

Inman, D.L. and Bagnold, R.A., 1967. Littoral Processes. In: M.N. Hill (Editor), The Sea, Interscience, New York, vol. 3: 529-553.

Isaacson, M., 1991. Measurement of Regular Wave Reflection. Journal of Waterway, Port Coastal and Ocean Engineering, ASCE, vol. 117, No. 6: 553-569.

Kawata, Y. and Tsuchiya, M., 1986. Applicability of Sub-sand System to Beach Erosion Control. Proc. Coastal Engineering Conference, Taipei, Taiwan, vol. 2: 1255-1267.

King, C.A.M., 1972. Beaches and Coasts, 2nd Edition. St. Martin's Press, New York, New York.

Krumbein, W.C. and Monk, G.D., 1942. Permeability as a Function of the Size Parameters of Unconsolidated Sand. American Institute of Mining and Metallurgical Engineers, vo. 142, Paper No. 1492: 1-11.

Longuet-Higgins, M.S., 1983. Wave set-up, Percolation and Undertow in the Surf Zone. Proc. Royal Society of London A, vol. 390: 283-291.

Longuet-Higgins, M.S., 1972. Recent Progress in the Study of Longshore Currents. In 'Waves on Beaches', Edited by R. E. Meyer, Academic Press, New York: 203-248.

Longuet-Higgins, M.S. and Parkin, D.W., 1962. Sea Waves and Beach Cusps. The Geographical Journal, vol. 128: 194-201.

Longuet-Higgins, M.S. and Stewart, R.W., 1962. Radiation Stress and Mass Transport in Gravity Waves, with Application to 'Surf Beats'. Journal of Fluid Mechanics, vol. 13: 481-504.

Longuet-Higgins, M.S. and Stewart, R.W., 1964. Radiation Stresses in Water Waves; a Physical Discussion, with Applications. Deep-Sea Research, vol. 11: 529-562.

Longuet-Higgins, M.S. and Stewart, R.W., 1960. Changes in the form of Short Gravity Waves on Long Waves and Tidal Currents. Journal of Fluid Mechanics, vol. 8: 565-583.

Machemehl, J.L., Thomas, J.F. and Norden, E.H., 1975. New Method for Beach Erosion Control. Civil Engineering in the Oceans, vol. 1: 142-160.

Madsen, O.S., 1978. Wave-induced Pore Pressure and Effective Stress in a Porous Bed. Geotechnique, vol. 28, No. 4: 377-393.

Mansard, E.P.D. and Funke, E. R., 1980. The Measurement of Incident and Reflected Spectra Using a Least Squares Method. Proc. 17th Coastal Conference, Sydney, Australia, vol. 1: 154-172.

Mase, H., 1994. Uprush-Backrush Interaction Dominated and Long Wave Dominated Swash Oscillations. Proceedings of the International Symposium: Waves - Physical and Numerical Modelling, Vancouver, British Columbia, vol. 3: 326-325.

McLean, R.F. and Kirk, R.M., 1969. Relationships Between Grain Size, Size-sorting, and Foreshore Slope on Mixed Sand-shingle Beaches. New Zealand Journal of Geology and Geophysics, vol. 12: 138-155.

McDougal, W.G., Kraus, N.C. and Ajiwibowo, H., 1994. Simulation of Wave and Beach Profile Change in Supertank Seawall Tests. Coastal Dynamics '94, Barcelona, Spain: 278-295.

Mei, C.C. and Foda, M.A., 1981. Wave-induced Responses in a Fluid-filled Poro-elastic Solid with a Free Surface - a Boundary Layer Theory. Geophysical Journal Royal Astronomical Society, vol. 66: 597-631.

Moshagen, H. and Torum, A., 1975. Wave Induced Pressures In Permeable Seabeds. Journal of the Waterways Harbors and Coastal Engineering Division, ASCE, vol. 101: 49-57.

Ogden, M.R. and Weisman, R.N., 1991. Beach Stabilization Using Drains - an Experimental Model Study. Coastal Sediments '91, Seattle, Washington, vol. 2: 1955-1969.

Ovesen, N.K. and Schuldt, J.C., 1992. Beach Management System Documentation. Report Number 300-01414. Danish Geotechnical Institute, Lyngby, Denmark.

Packwood, A.R., 1983. The Influence of Beach Porosity on Wave Uprush and Backwash. Coastal Engineering, vol. 7: 29-40.

Packwood, A.R. and Peregrine, D.H., 1980. The Propagation of Solitary Waves and Bores Over a Porous Bed. Coastal Engineering, vol. 3: 221-242.

Putnam, J.A., 1949. Loss of Wave Energy Due to Percolation in a Permeable Sea Bottom. Trans. American Geophysical Union, vol. 30, No. 3: 349-356.

Putnam, J.A. and Johnson, J.W., 1949. The Dissipation of Wave Energy by Bottom Friction. Trans. American Geophysical Union, vol. 30, No. 1: 67-74.

Quick, M.C. and Dyksterhuis, P., 1994. Cross-shore Transport for Beaches of Mixed Sand and Gravel. Proceedings of the International Symposium: Waves - Physical and Numerical Modelling, Vancouver, British Columbia, vol. 3: 1443-1452.

Quick, M.C., 1991. Onshore-offshore Sediment Transport On Beaches. Coastal Engineering, vol. 15: 313-332.

Quick, M.C. and Har, B.C., 1985. Criteria For Onshore-Offshore Sediment Movement On Beaches. Proc. Canadian Coastal Conference, St. John's, Newfoundland: 257-269.

Sakai, T., Hatanaka, K. and Mase, H., 1992a. Wave-Induced Effective Stress in Seabed and Its Momentary Liquefaction. Journal of Waterway, Port, Coastal, and Ocean Engineering, ASCE, vol. 118, No. 2: 202-206.

Sakai, T, Mase, H., Cox, D.T. and Ueda, Y., 1992b. Field Observations of Wave-induced Transient Porewater Pressures in Seabed. Proc. 23rd International Conference on Coastal Engineering, Venice, Italy, Paper No. 197: 407-408.

Savage, R.P., 1958. Wave Run-up on Roughened and Permeable Slopes. Journal of the Waterways and Harbors Division, ASCE, vol. 84, No. 3, Paper 1640: 1-37.

Sleath, J. F. A., 1984. Sea Bed Mechanics. Wiley, New York, New York.

Shore Protection Manual, 1984. Coastal Engineering Research Center, 4th Edition. U.S. Government Printing Office, Washington, DC 20402.

Sunamura, T., 1984. Quantitative Predictions of Beach-Face Slopes. Geological Society of America Bulletin, vol. 95: 242-245.

Walsh, B.W., 1989. Onshore/Offshore Transport Mechanisms. Master of Applied Science Thesis, The University of British Columbia.

Weisman, R.N., Seidel, G.S. and Ogden, M.R., 1995. Effect of Water-Table Manipulation on Beach Profiles. Journal of Waterway, Port, Coastal, and Ocean Engineering, ASCE, vol. 121, No. 2: 134-142.

Whitham, G.B., 1962. Mass, Momentum and energy Flux in Water Waves. Journal of Fluid Mechanics, vol. 12: 135-147.

Williamson, D.C. and Hall, K.R., 1992. Prediction of External Wave Pressures on a Rubble Mound Breakwater. Canadian Journal of Civil Engineering, vol. 19: 639-648.

Yamamoto, T., 1978. Sea Bed Instability from Waves. Proc. 10th Annual Offshore Technology Conference, Paper No. 3262, vol. 1: 1819-1827.